Universidade de Aveiro Departamento de Engenharia Mecânica
2019

João Pedro Menezes Andias

Incorporation of nanomaterials to customise recycled thermoplastics for applications in additive manufacturing

Incorporação de nanomateriais para customização de termoplásticos reciclados para aplicações em fabrico aditivo

Universidade de Aveiro Departamento de Engenharia Mecânica
2019

João Pedro Menezes Andias

Incorporation of nanomaterials to customise recycled thermoplastics for applications in additive manufacturing

Incorporação de nanomateriais para customização de termoplásticos reciclados para aplicações em fabrico aditivo

Dissertação apresentada à Universidade de Aveiro para cumprimento dos requisitos necessários à obtenção do grau de Mestre em Engenharia Mecânica, realizada sob orientação científica de Victor Fernando Santos Neto, Professor Auxiliar do Departamento de Engenharia Mecânica da Universidade de Aveiro, e de João Alexandre Dias de Oliveira, Professor Auxiliar do Departamento de Engenharia Mecânica da Universidade de Aveiro.

Esta dissertação teve o apoio dos projetos UID/EMS/00481/2019-FCT - FCT - Fundação para a Ciência e a Tecnologia; e CENTRO-01-0145-FEDER-022083 - Programa Operacional Regional do Centro (Centro2020), através do Portugal 2020 e do Fundo Europeu de Desenvolvimento Regional

O júri / The jury

Presidente / President

Doutora Paula Alexandrina de Aguiar Pereira Marques
Equiparada a Investigadora Principal, Universidade de Aveiro

Doutora Maria Alexandra Lopes da Fonseca
Engenheira de Investigação, Lynx - Advanced Composites, Lda (arguente principal)

Prof. Doutor João Alexandre Dias de Oliveira
Professor Auxiliar do Departamento de Engenharia Mecânica (co-orientador)

Agradecimentos / Acknowledgements

Part of the journey is the end, and in this end phase i would like to remember each step of this journey, sincerely saying a big thank you to everyone who contributed in way to the realisation of this work and the entire academic adventure of this young fellow. To my advisors, Professor Victor Neto and Professor João Oliveira, for their availability and guidance throughout the work, all the advice given and, most importantly, for all the cheerful and relaxed environment they provided, which meant a big boost in confidence and effort put into the work. To Tiago and Mylene for always giving a helping hand in dire times, being present to assist with any experiment, to give important recommendations and resources regarding the work and never forgetting to smile and cheer to relieve some pressure when the work starts to be tiresome. To Diana Fidalgo for helping with the DSC runs, to Ricardo Beja for the help with the tensile tests and Nuno Almeida for supplying the freeze-dried carbon nanotubes, as their help was invaluable to the completion of this work, always being ready to assist in whatever way they could. To my closest family, the ones who endlessly support me until the end of time, the ones who are always there to give me the strength i need to surpass any obstacle, contributing to a positive mindset even when facing the toughest challenge. To my closest friends, for all the good academic times we spent together, every conversation, every night out, for each and every good vibe that managed to brighten up even the cloudiest days, whether it was at the library, the laboratory or the canteen. To everyone not mentioned in this segment but whose presence always made my spirit rekindle with joy and willingness to continue working to finish my academic journey on a high. A big thank you to whom it may concern.

Palavras-chave

Ácido Poliláctico (PLA); Termoplástico; Nanotubos de Carbon; Fabrico Aditivo (AM); Fabrico por Filamento Fundido (FDM); Nanocompósito.

Resumo

Tendo já provas dadas no fabrico de prototipagem, o fabrico aditivo revela-se como uma tecnologia capaz de produzir componentes funcionais para as diversas áreas de engenharia. Os materiais termoplásticos apresentam propriedades que permitem conferir ao produto fabricado características que asseguram o seu correto funcionamento e a sua reutilização, assegurando o ciclo de vida do produto. Com a evolução da nano engenharia, tem-se vindo a utilizar diversos produtos baseados na inserção de nano particulas em determinados materiais de modo a conceber novas propriedades nunca antes obtidas. Obtendo provetes consituídos por Ácido Poliláctico através de fabrico por filamento fundido em impressão 3D, analisou-se as suas propriedades mecânicas mediante os resultados dos respetivos ensaios de tração. Analogamente, foram produzidos provetes constituídos por Nanotubos de Carbono que posteriormente foram também submetidos a testes de tração. Tendo obtido os resultados para cada tipo de material, fez-se uma análise e comparação entre cada um com o intuito de compreender como evolui o material após a mistura com um nanomaterial, retirando as conclusões necessárias acerca da evolução que estas modificações ao material proporcionam e da sua utilização futura e procurando aspetos de melhoria do processo geral para eventuais trabalhos futuros.

Keywords Poly-Lactide Acid (PLA); Thermoplastic; Multi Wall Carbon Nanotubes (MWCNT); Additive Manufacturing (AM); Fused Deposition Manufacturing (FDM); Nanocomposite.

Abstract Having shown evidences in prototype fabrication, Additive Manufacturing reveals itself as a technology capable of producing functional components for the various areas of engineering work. The thermoplastic materials have properties which grant the fabricated product characteristics that ensure their correct usage and recycle, preserving its life cycle. With the evolution of nanoengineering, several products based on the insertion of nanoparticles have been implemented and used in various applications, as they were granted new and better properties, never before been able to obtain. After acquiring Poly-Lactide Acid specimens through fused deposition modelling in 3D printing, they were submitted to tensile tests in view of analysing their mechanical behaviour. The same process was done to the thermoplastic material mixed with Carbon Nanotubes which were submited to tensile tests as well. Having obtained the results for both types of material, it was conducted an analysis and comparison between each one with the intention of comprehending how the material evolves after being mixed with a nanomaterial, drawing afterwards the necessary conclusions as to the evolution of said modifications in the thermoplastic in study and its future use, and seeking ways of improving the general process to be used in eventual future works.

Contents

List of Tables

List of Figures

Chapter 1

Framework

1.1 Introduction

Since the birth of the Additive Manufacturing industry, it has been expanding at a fast rate and for the past years it has been gaining a significant growth in terms of usage in the general production industry and in terms of popularity. What was once regarded as being restricted to just rapid prototyping, it has been continuously evolving to the point where it can also create fully functional components to be used in the industry such, as automotive. This technology has also captured significant media attention and gathered interest among the traditional manufacturing industries, as it comes with several advantages such as the possibility of producing extremely customised parts with a certain degree of complexity, in an economic and sustainable way, meeting the companies expectations of reducing the general production costs while enhancing the product quality and time efficiency.

1.2 Motivation

Being a relatively new technology it is somewhat interesting to study how to enhance the resulting products, what kind of materials and mixing elements should be added to the original base material in order to give it better properties for various areas of work. Of course, being available for common use, upgrading them can also be of an interest to the common 3D printer, as they can have faster access to a certain component needed for a more personal project. Regarding the materials used for Additive Manufacturing, investigating how they behave both mechanically and thermally, before and after mixing with another material, can provide useful insight for other projects regarding these types of plastic, as well as how the adding materials influence the plastic's behaviour and if such implementation is worthwhile.

1.3 Objectives

The prime objective of this work is to assess the evolution of Poly-Lactide Acid (PLA) samples obtained through Fused Deposition Modelling after being mixed with carbon nanotubes. After obtaining the intended results, it will be conducted an analysis on all the experiment stages of this work in order to try to justify any eventual discrepancy

between results, whether or not they demonstrate an improvement of the mechanical properties of the sample. The resulting investigation will consist of an equally important objective that complements the assessment previously mentioned as the main objective. Secondary objectives for this work consist of safeguarding the material's state, being it grain or filament. By means of analysing the plastic's heating cycle using a Differential Scanning Calorimetry (DSC), it can be assured that the grains are being dried correctly. Regarding the filament, it's apparent form throughout the extrusion process must be taken into consideration so that it suits the printer's requirements. When conducting the experiment phase, fulfilling all the mentioned goals translates into a more robust and reliable work, as it is developed in a much more controlled and supervised environment.

1.4 Work Guideline

The general document structure is comprised of four major chapters with each one giving an unique approach. The state of the art review will give a theoretical insight on all the technologies, processes and materials surrounding this work's environment, giving a basis on how to proceed in the experimental phase. The experimental work follows the state of the art review, informing how the procedure was conducted from the very first steps until the final tests, also giving information on every precautionary measure taken during a specific production phase. The experimental results chapter features all the tensile test results, showcasing the stress-strain graphic curves and the specific values registered. Afterwards, a section of discussion is present, consisting in a deep analysis regarding the nature of said results. To round up the document structure, a chapter giving the final remarks is presented, reviewing the work as a whole, including an insight on how future projects can be conducted and similar areas that can be explored via an investigation and research study.

Chapter 2

State of the Art

In this chapter it is presented the state of the art of all the technology associated with this work. It starts by giving the general definitions of Additive Manufacturing, its advantages, limitations and applications, focusing more specifically on Fused Deposition Modelling afterwards. Next, a section regarding a Differential Scanning Calorimetry is present, which describes its functionality, advantage of use and result display, as the process has been proven to be extremely informative in the experimental approach and in the veracity of the parameters used on certain phases of the work. The chapter ends by describing the materials used throughout this work, and the use of the freeze drying technic or lyophilisation as a useful process to dry the nanomaterials.

2.1 Additive Manufacturing

Additive manufacturing (AM), also known as 3D printing, uses computer-aided design to build objects layer by layer. The usage of this terminology is under the jurisdiction of Committee F42 on Additive Manufacturing Technologies [1]. After reaching a mutual agreement with the American Society for Testing and Materials (ASTM), the Society of Manufacturing Engineers (SME) provided the insight and technical expertise of its RTAM Community members to serve as the foundation and base rules of this standard. Nowadays, SME continues to play a pivotal role in advising and providing important guidance to most of the ASTM standards and their development [1].

This form of fabrication method contrasts with more traditional ones, as most of their processes such as cutting and drilling, grind away unwanted excess from a solid piece of material, often metal, giving origin to unnecessary waste, not utilising the full potential of a given material. The increasing amount of new equipment, technologies, and materials in AM are driving down the costs of building parts, devices, and products in industries such as aerospace, medicine, automotive, consumer products, and more [2]. Figure 2.1 shows schematically this difference between both forms of fabrication.

The general advantages of additive manufacturing when compared to traditional manufacturing are the capabilities in design and development of products. Despite certain limitations, companies are using AM increasingly to use the many possible benefits like complexity-for-free manufacturing. When we look at traditional manufacturing, the more complex the product is, the more it will cost. Being fabricated with a more degree of precision, it requires more energy and time to produce the pretended object or

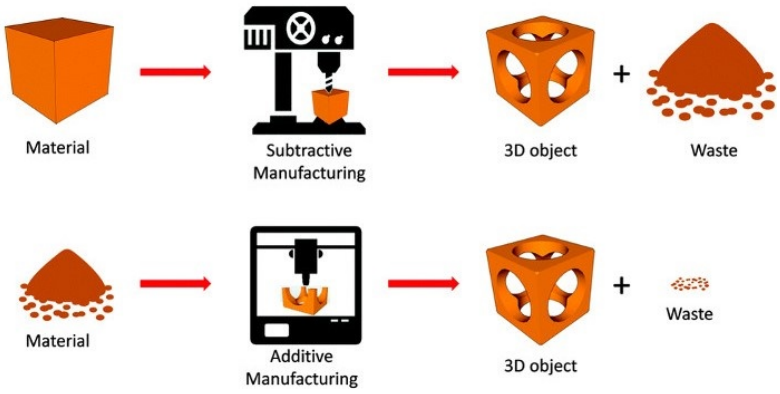

Figure 2.1: Schematic representation of the differences between Additive and Subtractive Manufacturing in terms of material waste (adapted from [3]).

product. It can be said that, in this situation, there exists a direct connection between complexity and manufacturing costs [4], one key aspect that does not occur in AM.

Despite the product in hand having a relative moderate complex rate, in AM there is no limitation when it comes to higher costs for higher complex objects, as well as there is no need to produce or purchase auxiliary tools to help in the fabrication stage. The same logic can be applied to the design stage, as there is a moderate to high concern regarding the costs in construction of said product, thus its design being heavily limited. The greater freedom of design via AM makes it possible to combine an assembly of parts into one part and, therefore, to reduce the required assembly work and costs [4].

Another key aspect is that AM, unlike traditional manufacturing processes, does not need a strict user involvement, as the machines can operate independently, meaning that the production of components will require a minimum of operator involvement. During part building, the various machines systems do not require any input from the operator, as systems require no input from said operators. This alone creates an impact on the manner in which a manufacturing environment operates, giving the users the liberty to work on other machines and making it flexible and feasible for parts to be built overnight or at weekends when traditional manufacturing companies would need to either halt production or increase workers pay rates at these times. As such, the total number of production hours of the machines is increased without the need to move to shift patterns in order to have skilled machine operators on site. Thus, the majority of costs will result from the machine, its capital cost, energy consumption and usage [5].

AM is more and more often, not only used for rapid prototyping but for the production of ready made elements and for making functional and durable products [6]. Incremental production is increasingly used in the performance of functional and durable products. Currently five out of ten printed elements are ready made products [7]. Wherever there is a variety of products, individuality of production and short-run, incremental production is the solution. Industrial design, medicine, aviation and the armaments industry take advantage of the advantage of incremental manufacturing systems in the performance of fully usable products [7].

Medicine is one of the most important and notorious areas that AM products can be pivotal in terms of availability and time to be fabricated, granting the possibility of having specific designs products fit determined body parts such as some prosthesis. With the

aim to assist, maintain or restore a person´s mobility, doctors need custom-made design implants which are less in number and differ from patient to patient. Additive manufacturing fulfils this need efficiently and products are quickly available and produced at an economical price [8]. Table 2.1 summarises the several applications in medicine.

Table 2.1: Applications of AM in medicine, adapted from [8]

Criteria	**Achievement**
Designing and manufacturing of surgical aid tools, bio-models and implants.	·Play a useful role for design and production of surgical support tools, bio-models and implants; ·Used for the surgical tools up gradation.
Designing and manufacturing of various scaffolds for tissue engineering.	·An AM characteristic is to design and manufacture the different scaffolds for the restoration of tissues; ·It replaces conventional scaffold fabrication methods; ·AM help for printing organs, produced cells, cell-laden biomaterials, biomaterials individually.
Development of various medical devices and surgical training models.	·Used for developing various medical models, surgical training models which are used in medical education.
Individualisation	·AM is used for individualisation, as data differs from patient to patient; ·Used for customised implant fabrication.
Complex Geometry	·This technology has great potential for fabrication of complex geometries implant.
Functional integration	·The medical models are in functional integration; ·It works like an original one.
Reduced costs	·AM technology helps for reducing cost of medical implant as compared to other manufacturing processes.
Rapid availability	·AM has availability for producing medical model in short time.
Improved patient care	·This technology is used for development and improve patient care through the customised model.
Cost-effectiveness for the hospital	·AM technology makes possible to manufacture customised implants which comfortably fit the patient with reasonable cost.
Weight reduction	·Reduction of weight done with the help of this technology by changing material.

The aerospace industry continues to find new applications for additive manufacturing. One area of focus shared by a variety of aerospace companies is the creation of engines using 3D printing techniques, and this is true from jet turbines to rocket engines. In April 2016, General Electrics (GE) sent the first two production run LEAP-1A engines to Airbus with 19 3D printed nozzles included. LEAP engines using these nozzles are approximately 15 percent more fuel efficient than their counterparts [9]. At the end of December 2016, another major step forward was achieved for LEAP engines and their 3D-printed nozzles. The LEAP-1C jet engine was approved by the Federal Aviation Administration (FAA) and the European Aviation Safety Association (EASA) [9].

Regarding safety, there are numerous of practical applications of these polymer lattices that were developed by different researchers and industries for the Head Health Challenge [10] organised by GE and the National Football League (NFL) for improving the safety of NFL players on the football field. In particular, the best helmet for protection from the impact was prototyped using AM techniques [10; 11].

Table 2.2 shows a resume of the most common used materials and their respective applications in Additive Manufacturing, pointing out the benefits and challenges carried out for each affinity.

Table 2.2: Resume of AM applications, adapted from [10]

Materials	Main applications	Benefits	Challenges
Metals Alloys	·Aerospace; ·Automotive; ·Military; ·Biomedical.	·Multifunctional optimisation; ·Mass-customisation; ·Reduced material waste; ·Fewer assembly components; ·Possibility to repair damaged or worn metal parts.	·Limited selection of alloys; ·Dimensional inaccuracy; ·Poor surface finish; ·Post-processing may be required (machining, heat treatment, etc).
Polymers Composites	·Aerospace; ·Automotive; ·Sports Medical; ·Architecture; ·Toys; ·Biomedical.	·Fast prototyping; ·Cost-effective; ·Complex structures; ·Mass-customisation.	·Weak mechanical properties; ·Limited selection of polymers; ·Anisotropic mechanical properties (in fibrereinforced composites).
Ceramics	·Biomedical; ·Aerospace; ·Automotive; ·Chemical industries.	·Controlling porosity of lattice; ·Printing complex structures; ·Printing scaffolds for body organs; ·Reduced fabrication time; ·A better control on composition.	·Limited number of printable ceramics; ·Dimensional inaccuracy; ·Poor surface finish; ·Post-processing may be required.
Concrete	·Infrastructure; ·Construction.	·Mass-customisation; ·No need for formwork; ·Less labour required; ·Useful in harsh environments such as space construction.	·Layer-by-layer appearance; ·Anisotropic mechanical properties; ·Poor inter-layer adhesion; ·Difficult application to larger buildings; ·Limited number of printing methods, concrete mixture design.

2.2 Fused Deposition Modelling

The technology behind Fused Deposition Modelling (FDM) was invented by Scott Crump, CEO of Stratasys. The term FDM is trademarked by Stratasys. At least one of the patents issued to Mr. Crump has expired, enabling companies like RepRap to use that knowledge to develop their versions of extrusion systems. RepRap coined the term fused filament fabrication to avoid trademark conflicts [12].

In the physical process of fabrication, a plastic filament is fed through a heating element and becomes semi-molten. It is then fed through a nozzle and deposited onto the print bed or the partially constructed part already being produced. At this phase, since the material is extruded in a semi-molten state, the newly deposited material fuses with adjacent material that has already been deposited onto the print bed. The head containing all the extrusion components then moves around in the X-Y plane and deposits material according to the part geometry defined by the user previously. After depositing the intended layer in the X-Y plane, the platform moves vertically along the Z axis to begin depositing a new layer on top of the previous one [13]. After a period of time, the head will have deposited a full physical representation of the original CAD file. The time taken to produce a full fledged piece depends on the printing parameters set by the user, being the extrusion speed the major contributor.

The extruder, arguably the most complex part of a 3D printer that is still seeing intense development, is actually the marriage of two key elements: the filament drive and the thermal hot end. The filament drive pulls in plastic filament often bundled in spools of either 3mm or 1.75mm diameter filament using a geared driver mechanism. The hot end usually is thermally insulated from the rest of the extruder and is made up of either a large block of aluminium with an embedded heater or some other heater core, along with a temperature sensor [14]. Another key component of a FDM 3D printer is

the print bed which is used to prevent warping or cracking of prints as they cool and to create better adhesion between the first layers of the print and the print bed surface. The surface of the print bed is often made from either glass or aluminium to better spread the heat across the area and to make for a smooth and level surface. Glass provides the smoothest surface to print on while aluminium conducts heat better for a heated platform. To prevent the object from lifting off the surface in mid-print, these surfaces are often covered in one kind of tape or another to provide a surface that is inexpensive to replace periodically [14]. Figure 2.2 represents the general components of the FDM process, while a printing is being executed.

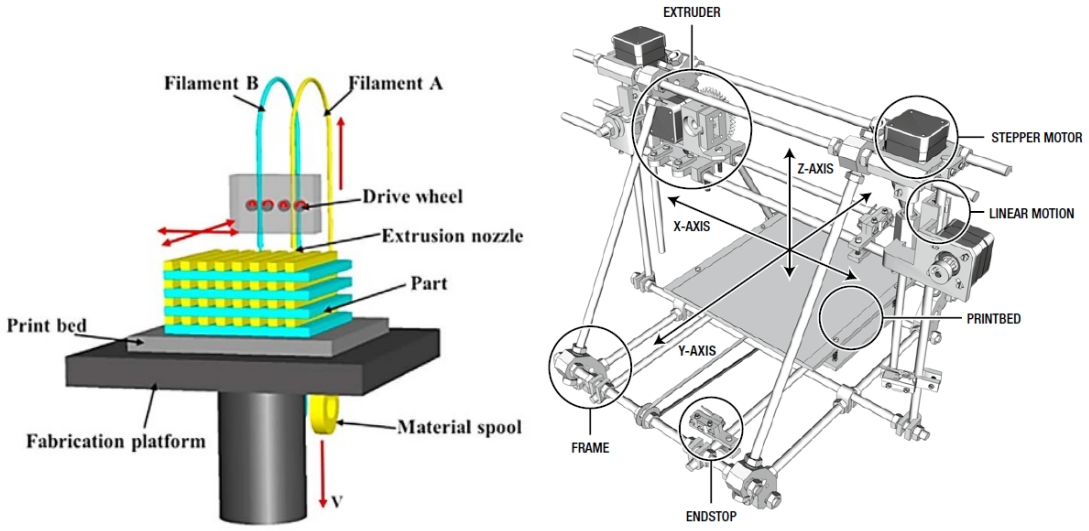

(a) (b)

Figure 2.2: Representation of the FDM process and its general components (adapted from [13]).

An advantage of this system is that it may be viewed as a desktop prototyping facility in a design office since the materials it uses are cheap, non-toxic, non-smelly and environmentally safe. There is also a large range of colours and materials available, such as investment casting wax, ABS plastic, medical grade ABS (MABS) and elastomers [15]. All produced parts made by using this method have a high stability since they are not hygroscopic [16].

Despite the numerous benefits of the FDM process, it is yet encompassed with various kinds of setbacks such as poor surface quality, strength of products etc. The poor surface quality observed in the end products of the FDM process was largely due to the layer upon layer deposition of the building process. Investigations have confirmed that there are three types of surface textures in the FDM prototypes. The bottom surface is made up of the first deposited layer, which is usually in direct contact with the printing platform or support material. Hence, it picks up the surface texture of the build platform (or the support material which had been deposited already). Similarly, the top layer is the last layer to be deposited, it usually consists of a ridged surface which results from the structure of the strands of the modelling material. The third texture observed was the middle surface which takes the rough texture of the layer upon layer pattern [17].

Table 2.3: Fused Deposition Modelling description

Process	Materials	Applications	Benefits	Drawbacks
Fused Deposition Modelling	·Continues filaments of thermoplastic polymers; ·Continuous fibre-reinforced. polymers	·Rapid prototyping; ·Toys; ·Advanced composite parts.	·Low cost; ·High speed; ·Simplicity.	·Weak mechanical properties; ·Only using thermoplastics; ·Layer-by-layer finish.

2.3 Differential Scanning Calorimetry

Differential scanning calorimetry (DSC) is an experimental method that directly measures the difference in heat energy uptake taking place in a sample relative to a reference during a regulated temperature change. DSC is a technique in which the difference in the amount of heat required to increase the temperature of a sample and reference are measured as function of temperature. It is applicable to a variety of materials including polymers, pharmaceuticals, foods and inorganics. DSC measurements provide qualitative and quantitative information as a function of time and temperature regarding transitions in materials that involve endothermic or exothermic processes, or changes in heat capacity [18].

In heat flux DSC, the difference in heat flow into the sample and reference is measured while the sample temperature is changed at the constant rate [19]. The main assembly of the DSC cell is enclosed in a cylindrical, silver heating black, which dissipates heat to the specimens via a constantan disc which is attached to the silver block. The disk has two raised platforms on which the sample and reference pans are placed. A chromel disk and connecting wire are attached to the underside of each platform, and the resulting chromel-constantan thermocouples are used to determine the differential temperatures of interest. Alumel wires attached to the chrome discs provide the chromel-alumel junctions for independently measuring the sample and reference temperature [20]. Figure 2.3 represents the general components of a DSC machine.

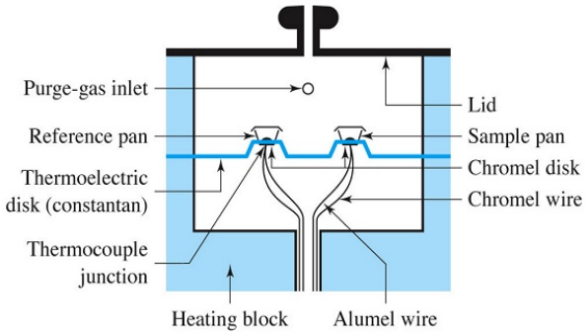

Figure 2.3: Differential Scanning Calorimetry machine representation and integral components (adapted from [20]).

Some of the advantages contributing to the widespread usage of DSC are the ease of sample preparation, the applicability to both solids and liquids, fast analysis time and wide temperature range. it is not without limitations. First, the baseline subtraction step introduces some form of human inconsistency into the raw data analysis; thus, variations in results may be observed among different users. Second, differential scanning calorimeters have minimum concentration limits which might be difficult to achieve at

bulk manufacturing scale. Third, the enthalpy of irreversible thermal denaturation is not absolute; which implies that the derived Gibbs free energy, which is an indicator of protein stability, in similar scenarios can be misleading. Furthermore, the method works best for purified samples. Presence of impurities may either cause a shift in the melting temperature, T_{m}, if there is an interaction with the protein under investigation, or appearance of new thermal transitions if there is no interaction. In any case these extra features on the thermograms can be wrongly attributed to samples, thus impacting the interpretation of results [21].

The results of a DSC scan are commonly obtained in the form of two curves, representing the heating and stages of the process. In the point of view of the sample, it can be replaced the terms 'heating' and 'cooling' by the type of reaction process that occurs, them being endothermic and exothermic respectively. The general shape of the curve is represented in figure 2.4. Polymer samples, whose melting curves are concave in shape, are characterised by the temperatures of their peak maxima. Another important aspect of the DSC curve is the study of the type of material used regarding its crystalline structure. For example, still concerning the endothermic phase, partially crystalline polymers give rise to very broad melting peaks because of the size distribution of the crystalites [22]. Another way to characterise ones structure is to study its glass transition via the glass temperature. A glass transition always requires the presence of a certain degree of disorder in molecular structure of material under investigation, being very sensitive to changes in molecular interactions. Its measurement can be used to determine and characterise structural differences between samples or changes in materials [22].

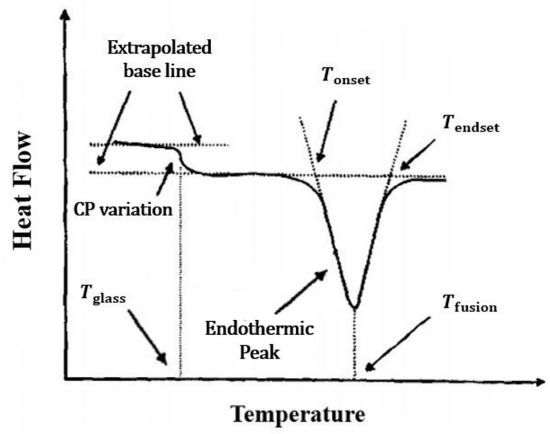

Figure 2.4: General DSC graphic representation (adapted from [22]).

2.4 Materials Used

2.4.1 Poly-lactide Acid

Poly-lactic acid (PLA) is a highly versatile, biodegradable, aliphatic polyester derived from 100 per cent renewable resources, such as corn and sugar beets. Its basic monomer is lactic acid, which is derived from starch by fermentation and it is a sustainable alternative to petrochemical-derived products, since the lactides produced from agricultural by-products mainly the carbohydrate rich substances [23].

In addition, its properties are comparable to, or even better than, those of petroleum-based polymers, such as polyethylene (PE), polypropylene (PP), polystyrene (PS), polycarbonate (PC), and polyethylene terephthalate (PET). For example, compared with PS, PLA shows high strength and toughness, as well as low permeability performance against the transfer of several gases such as water vapor and methane. At the beginning of the development of PLA, special attention was given to develop new methods and techniques of polymerisation for achieving high-molecular-weight PLA materials. Indeed,the ring-opening polymerisation (ROP) of lactide monomers was used to synthesise PLA materials with high molecular weights (greater than approximately 100,000 g/mole) and improved properties [24].

Due to its bioresorbability and biocompatibility in the human body, lactic acid-based polymers have been used for resorbable sutures and prosthetic devices [25]. PLA has been finding increasing consumer applications mainly due to its renewability, biodegradability, transparency, processibility, and mechanical properties. Although PLA has been shown to be a practically feasible packaging material, its higher cost has confined its use to limited packaging application only [25]. Dannon and McDonald's (Germany) pioneered the use of PLA as a packaging material in yogurt cups and cutlery [25]. NatureWorks LLC polymers have been used for a range of packaging applications such as high-value films, rigid thermoformed containers, and coated papers. BASF's Ecovio®, which is a derivative of petrochemical-based biodegradable Ecoflex® and contains 45 wt percentage PLA, has been used to make carrier bags, compostable can liners, mulch film, and food wrapping. Commercially available PLA films and packages have been found to provide mechanical properties better than polystyrene (PS) and comparable to PET [25].

Like any other material, PLA comes with a series of advantages as well as certain limitations. Within the former, the general advantages centre around environment sustainability usage and production, making it an attractive bio polymer. Another key aspect, and one of the most attractive aspect of PLA, is its biocompatibility, being one of the best materials for implants in living organisms, including the human body. As a biocompatible material, it should not produce toxic or carcinogenic effects in local tissues and PLA degradation products are non-toxic (at a lower composition) making it a natural choice for biomedical applications. The following table points to several characteristic aspects of PLA. In addition, when compared with other biopolymers such as poly(hydroxyalkanoates) (PHAs), poly(ethyele glycol) (PEG) or poly(caprolactone) (PCL), it has a better thermal processability with its production requiring less energy output, making its production potentially advantageous with respect to cost. PLA can be processed by injection moulding, film extrusion, blow moulding, thermoforming, fiber spinning and film forming.

As for the later, PLA limitations centre around its structure, mechanically and chemistry wise. It demonstrates a poor toughness level, which limits its use in the applications that need plastic deformation at higher stress levels, despite showing promise regarding the tensile strength and elastic modulus when compared to other materials [25]. It is shown to be hydrophobic and to lack reactive side-chaingroups making its surface and bulk modifications a challenging task. Also, due to its low cell affinity, it can elicit an inflammatory response from the living host upon direct contact with biological fluids. Finally, its slow degradation rate is also to be considered as it is an important selection criterion for biomedical applications [33]. It degrades through the hydrolysis of

backbone ester groups and the degradation rate depends on several factors such as the PLA crystallinity, molecular weight, molecular weight distribution, morphology, water diffusion rate into the polymer and the stereoisomeric content. Table 2.4 describes all the advantages and disadvantages mentioned before.

Table 2.4: Advantages and disadvantages of the usage of PLA

Advantage	**Description**	**Reference**
Eco-Friendly	·It is biodegradable, recyclable, and compostable; ·Its production also consumes carbon dioxide.	[26],[27] [28]
Biocompatibility	·Hydrolyses when implanted in living organisms; ·Degradation products should not interfere with tissue healing; ·Degradation products are non-toxic at a lower composition.	[29],[30] [29] [29; 31]
Processibility	·Better thermal processibility compared to other biopolymers; ·Possibility of being processed by different processes.	[25] [25]
Energy Saving	·25% to 55% less energy to produce than petroleum-based polymers; ·Further reduced to less than 10% in the future.	[32] [32]
Disadvantage	**Description**	**Reference**
Poor toughness	·Very brittle with less than 10% elongation at break;	[34],[35]
Slow degradation	·Degrades through the hydrolysis of backbone ester groups; ·Depends on several factors that influence its degradation rate.	[36] [36]
Hydrophobicity	·Low cell affinity; ·Risk of an inflammatory response from the living host.	[37],[38] [37],[38]

2.4.2 Multi Walled Carbon Nanotubes

Before introducing the major content of this subsection, a general overview regarding nanomaterials and, in specific, carbon nanotubes must be given. According to the norm regarding nanotechnology, a nanoparticle can be defined as a particle with dimensions in the range of 100 nanometers or below. Therefore, a nanomaterial is a material which contains an element within the nanometric scale, whether it is an external, internal or even superficial structure [39]. Carbon nanotubes (CNTs) are a type of nanomaterials with the form of carbon. They were first discovered in 1952 in Russia, but mostly ignored, then rediscovered in the 1991 at NEC's Fundamental Research Lab in Japan as a minorby-product of fullerene synthesis [40]. During early analysis, CNTs have demonstrated to have very interesting mechanical properties, which instantaneously made them one of the most promising nanomaterials. On par with this, CNTs are both electrically and thermally conductive. Theoretically, metallic CNTs can conduct electricity with a current density of 4×109 A/cm^2, which is more than 1000 times greater than common metals such as copper [41]. The electrical properties of the tubes could change during deformation and stretching. The small size and highly symmetric structure allow for remarkable quantum effects and magnetic, electronic and lattice properties of CNTs [42].

Ebbesen et al. [43] confirmed experimentally that the electronic properties of nanotubes could vary widely from tube to tube: 25 both semiconducting and metallic behaviour has been observed. Measured resistivities fall into the approximate range of 0.05 mV·m to 10 mV·m. This compares with a value of approximately 0.4 mV·m for high quality single crystal graphite (parallel to the c axis) and 0.017 mV·m for copper.

The thermal and optical properties of carbon nanotubes have been studied less in-

tensively than the electronic properties, but some interesting results have been obtained. The high thermal conductivities of nanotubes have already been mentioned [44]. Regarding the thermal properties, it has been demonstrated that CNTs have at least twice the thermal conductivity of a diamond [45]. It has also been reported that carbon nanotube suspensions have non-linear optical properties, suggesting possible applications as optical limiters [44].

Having the basic knowledge regarding nanomaterials, and carbon ones in specific, it can now be analysed the version of CNT used in this work, the Multi-Wall Carbon Nanotubes (MWCNTs). While studying the properties of certain carbon nanotubes, its essential to know before hand its general structure, more notoriously if its the case of Single-wall Carbon Nanotubes (SWCNTs) or Multi-Wall Carbon Nanotubes (MWCNTs), as experimental procedures can divert from how many carbon layers the nanotube has. Focusing more on MWCNTs, they are hollow, cylindrically shaped allotropes of carbon that have a high aspect ratio (length to diameter ratio). Their name is derived from their structure and the walls are formed by multiple one-atom-thick sheets of carbon. Observed diameters range from 2 to 50 nm depending on the number of graphene tubes, and also feature an approximate inter-layer distance of 0.34 nm [47]. The MWCNTs observed by Iijima were produced at extremely high temperatures (near 3500°C) by use of an arc discharge between graphite electrodes [46]. Today, MWCNTs are produced industrially at temperatures ranging from 700°C to 950°C using the catalyst-based chemical vapor deposition (CVD) process developed by Endo and coworkers in the 1970s [44]. Scanning electron microscope (SEM) imaging is used to characterise the overall morphology of MWCNT samples, and could also be used to quantify the degree of purity within samples, as well as the dimensions of the tubules [48]. Figure 2.5 shows SEM images with two different magnifications with the corresponding nanotube model. Using a 'nanostressing stage' inside a SEM, it is indicated that the Young's modulus of the outermost layers of multi walled carbon nanotubes vary from 270 to 950 GPa. These measurements have also been carried out using atomic force microscopy (AFM) [43].

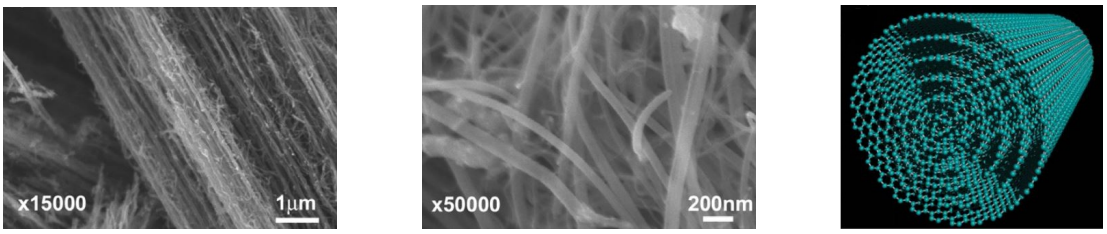

(a) (b) (c)

Figure 2.5: SEM representation of Carbon NanoTubes and molecular model (adapted from [48]): (a) SEM image with 15000× magnification, (b) SEM image with 50000× magnification, (c) molecular model of a six-walled carbon nanotube.

Various experiments were done with MWCNTs in order to test their mechanical aptitude, namely direct measurements of the bending forces as a function of the displacement using the already mentioned AFM. As reviewed in [49], Falvo et al. observed that MWCNTs could be bent at sharp angles without undergoing any structural fracturing and Zhu et al. applied high pressures values around 50 GPa at room temperature using shock waves, to arc-discharge MWCNTs and noted that the tubes do not break

but collapse, meaning that the outer shells transform into curled graphene domains while the inner cores display structural defects.

2.4.3 Polymer-matrix Nanocomposites

Having presented both of the materials used in this work, it is time to finally research the nature of the resulting material, being it a PLA nanocomposite, after mixing both PLA and the MWCNTs. But firstly, an insight to what a composite and a nanocomposite are needs to be given.

A composite material is a material made from two or more constituent materials with significantly different physical or chemical properties that, when combined, produce a material with characteristics different from the individual components. Composites are namely made up of two individual materials known as the matrix and the reinforcement. The matrix material surrounds and supports the reinforcement materials by maintaining their relative positions. The reinforcements impart their special mechanical and physical properties to enhance the matrix properties. The correct synergy between both materials produces properties unavailable from the individual materials, while the wide variety of matrix and strengthening materials allows the designer of the product or structure to choose an optimum combination. Examples of thermoset polymer matrices are epoxy resins and polyurethane and in the case of thermoplastics nylon, polycarbonate, polystyrene, polyethylene or, this work's material, PLA.

Nanocomposites are a subset of composites that utilise the unique properties of materials in the nano scale. The promising aspect of nanocomposites resides in its multifunctionality, having the possibility of creating unique combinations of properties intangible with traditional materials [50]. The composites ensure the size distribution and the subsequent dispersion of the nano components, and adaptation and understanding of the role of interfaces between the structurally or chemically phases, different in mass properties. More specifically regarding polymer-matrix nanocomposites, they contain an organic matrix in which inorganic nanomaterial is dispersed, resulting in enhanced optical, thermal, mechanical, magnetic and electronic properties due to the synergy of both organic and inorganic components [51]. Ajayan et al. [47] note that with polymer nanocomposites, properties related to local chemistry, degree of thermoset cure, polymer chain mobility, polymer chain conformation, degree of polymer chain ordering or crystallinity can all vary significantly and continuously from the interface with the reinforcement into the bulk of the matrix. With the upgrades to the newly made material, it was studied the application of these types of nanocomposites in biomedical applications, more specifically in developing biointerface controlling cell behaviours, biosensors for diagnosis, drug vehicles and wound dressings [52] and its potential in ultra purification applications [53].

Regarding more specifically a PLA nanocomposite based on carbon nanotubes, as reviewed in [54], and more recently in [55], there are three main methods used to obtain a dispersion of said nanoparticles into a PLA matrix, them being through solution mixing, melt blending, or in situ polymerisation. Focusing more on the melt blending process, which was the one used for this work, as it is mentioned by the review [55] it is economically attractive, environmentally friendly and a highly scalable method for preparing nanocomposites. For the melt blending process, attention needs to be given to the working condition, as a set of combination of parameters going from temperature to

rotation speeds can be implemented. Adjusting these parameters can alter the state of dispersion of the nanomaterials, such as the MWCNTs, within a PLA matrix. As such, using extrusion technology, Villmow et al. [56] studied the influence of these melt-mixing conditions in said scenario. The aim was to achieve a suitable distribution and dispersion of MWCNTs within the polymeric matrices to ensure low percolation thresholds, combined with high mechanical performance. Forwarding in the field of FDM, Postiglione et al. [57] studied the rheological behaviour of MWCNTs/PLA nanocomposites and their influence in the extrusion process. This was achieved through the analysis of the shear stress applied in the fused polymer when it goes through the extrusion nozzle. It was noted that, in the event of forming clusters, the dispersion of the nanoparticles may influence the deposition process of the fused material, leading to the clogging of the nozzle as well as influencing the way the material flows when extruded. It was also verified that the viscosity increased with the addition of the MWCNTs, not harming the material processing. As far as applications are concerned, several developments in packaging engineering and in tissue engineering were made possible, focusing in the synthesis of PLA nanoparticles, the processing of PLA based multifunctional nanocomposites and PLA surface modification techniques were conducted [58].

Before mixing MWCNTs with any polymer, PLA included, it is good practice to prepare it by cleansing it from any water remnants present in the samples. To achieve this, it can be used a freeze-drying technic or lyophilisation, which consists in removing water from a frozen sample by reducing the surrounding pressure with heating to provoke sublimation and desorption under vacuum conditions [59]. Lyophilisation can be used to enhance several material combinations, contributing for a reliable drying process while maintaining the particles alignment. Such was seen in [60] where this method improved the distribution of platinum nanoparticles in a SWCNT. While sublimating, there is a very weak link between the water molecules and the platinum nanoparticles, which greatly mitigates their agglomeration. Figure 2.6, represents a comparison between what would be a normal drying process and the lyophilisation in the case of the mentioned study.

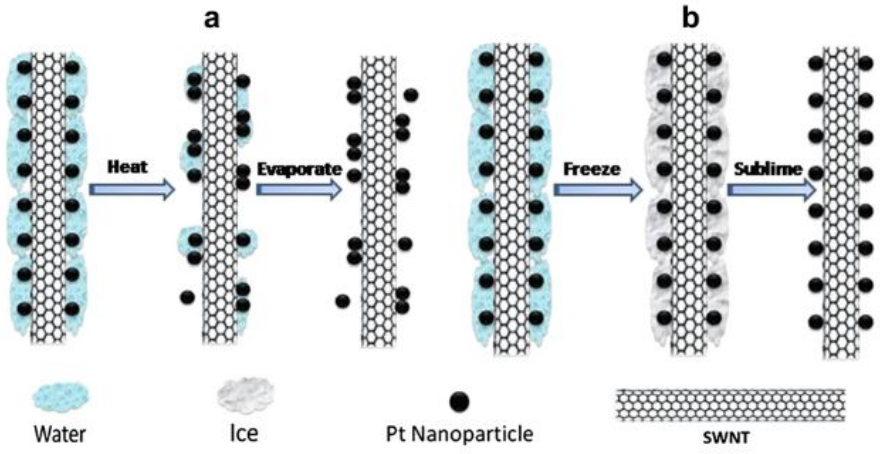

Figure 2.6: Schematic representation and comparison between a normal drying process (a) and the freeze drying process (b) (adapted from [60]).

As reviewed in [61] there are several applications for the lyophilisation process such

as improving colloidal nanoparticles' long-term stability, improving drug association to nanoparticles, preparing core/shell nanoparticles, producing solid dosage form and making an analytical characterisation of colloidal systems.

Chapter 3

Experimental Procedure

In the present section it is described the experimental procedure as well as an indication of all the parameters used in the work. Before the fabrication phase, a DSC scan was conducted for both the virgin and recycled PLA in an attempt to study their thermal behaviour during the heating stage of the thermal cycle, as well as confirming that the drying phase is being done correctly. After the scan, the work is divided into two major sections, in which the first one it is only used PLA as the sole thermoplastic material and the second one it is added an extra material to the mentioned PLA. In both sections, it takes place two phases of sample fabrication, with them being the filament production and sample printing. In the case of the recycled PLA it is presented an extra phase named the grain production. The study will not be complete without the results of the mechanical properties of every material produced, as it will be a key aspect of the work the respective tensile tests.

3.1 Thermoplastic Samples

Three samples of PLA were prepared for the work: commercial PLA (cPLA), virgin PLA (vPLA) and recycled PLA (rPLA). The cPLA was already provided in the form of filament by the company Leon3d, the vPLA was provided in the form of grain by the company Ercros and lastly the rPLA was provided in the form of remains of components from previous working assemblies in the industrial environment.

3.1.1 Drying Phase

The grain samples were heated in the stove at 50°C over 3 hours, with the purpose of reducing the humidity ratio. The presence of humidity within the samples can translate in an incorrect filament production, as its presence can affect the extrusion temperature and the flowability of the filament, as well as changing its surface properties.

3.1.2 DSC Scan and Results

In order to verify that the samples were being correctly dried, a grain from both the vPLA and the rPLA were submitted to a DSC Test. In addition, the corresponding results will indicate the correct range of temperature to be used throughout the experimental phase. As described in [62; 63], the melting temperature, T_{m}, would be around 175°C,

with the glass transition temperature, T_g, ranging from 55°C to 60°C. Since PLA can have various processing origins, it is always insightful and important to confirm these parameters before starting any experiment. The scan was conducted in a Discovery DSC 250 from TA Instruments represented in Figure 3.1. The DSC results were obtained and shown in the early stages in order to confirm the correct execution of this work, specifically the drying process.

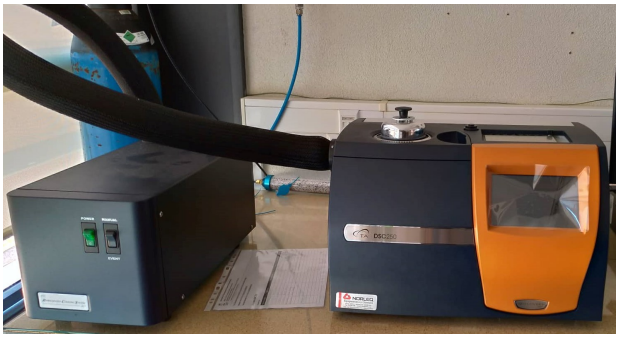

Figure 3.1: TA Instruments' Discovery DSC 250.

The heat flux DSC was conducted where the sample was heated from a single heating source. The temperature difference between the heating source and the sample is recorded and converted to a power difference. This power difference gives the difference in heat flow. In order to achieve the results desired for the analysis, it was enough to just work with a single heating phase, from a temperature of 9.9°C until the extrusion temperature of the printing process of the thermoplastic, 210°C, with a heating rate of 10°/min. After the completion of the DSC trial, the results were as shown in Figure 3.2.

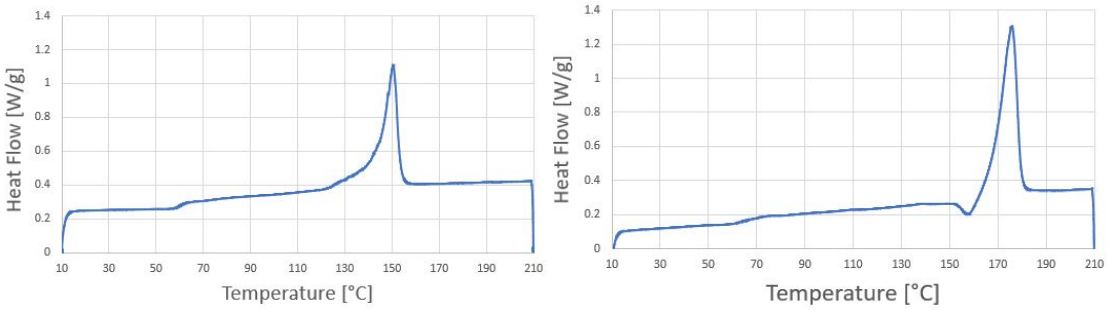

(a) (b)

Figure 3.2: DSC scan graphic results for the heating stage of the thermal cycle: (a) vPLA, (b) rPLA.

Following the corresponding literature [22], the vPLA sample result shown in Figure 3.2 (a) registers the melting temperature at the peak value of the heating stage. As for the glass transition temperature, in this sample is evident the 'S' curve at 60°C, keeping it true to what a newly produced PLA should have, as described in [62; 63]. Secondly, in the rPLA sample it can be noted, such as in the vPLA sample, the melting temperature at the peak value of the heating stage. Also, despite being with the slightest of margins, at around the 60°C mark where the curve adopts an 'S' form, it can

be registered the glass transition temperature of the PLA sample analysed. This value is assumed to be approximately the centre value of the 'S' curve, which in this case is around 68°C. This difference can be justified as the latter, being a recycled material, has already suffered changes due to thermal or mechanical strains, giving it other properties that diverge greatly from the former. Having confirmed the melting temperatures, it is safe to proceed to the following work stages, now knowing the correct temperatures to set. As explained further, this information will be essential to the extrusion phase, in respect to the quality of the filament extruded.

3.1.3 Grain Production

As described before, between the three types of PLA used, only the rPLA was subjected to the grain production. However, before one could start producing the grain, it was necessary to firstly crush the macro pieces provided. To achieve this desired objective, in a first stage, the pieces were cut into smaller ones using a 1.5 kW plastic grain crusher represented in Figure 3.3 (a), and in a latter one they were crushed in a small crusher machine, represented in Figure 3.3 (b). It was carefully measured the dimensions of the crushed particles, as they should have approximately 5×5×2.5 mm^3 in order to fit properly in the extruder.

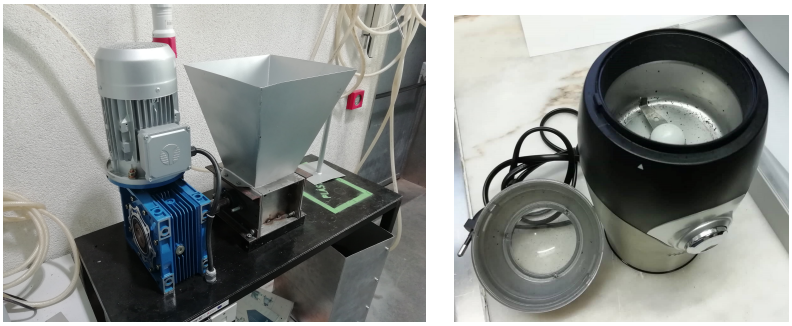

(a) (b)

Figure 3.3: Plastic grain crushers: (a) Plastic Grain Crusher, (b) Small Crusher.

3.1.4 Filament Production

Before being extruded, both vPLA and rPLA grain materials were submitted to a drying process, the same ones used to prepare the sample for the DSC scan. They were heated in the stove at 50°C over 3 hours. For the filament production, it was used the extruder Noztech Pro represented in Figure 3.4. The dried grain is deposited in the worm screw, and guided by it to the extrusion chamber, where the pretended filament is extruded. The extrusion temperature was always regulated depending on the state of the filament being extruded, in order to obtain sufficiently flexible filament at a constant speed with an uniform diameter in between 1.55 mm and 1.75 mm. For the vPLA the ideal temperature was 160°C, while for the rPLA was 180°C.

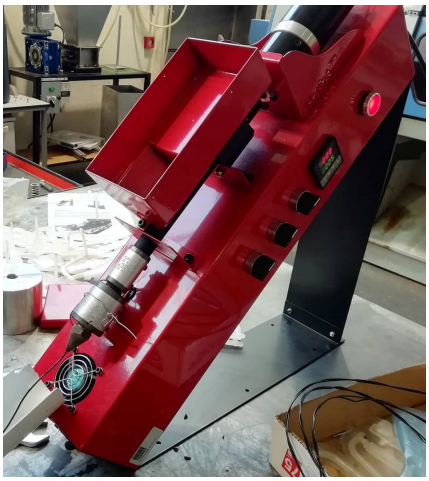

Figure 3.4: Noztech's Noztech Pro extrusion machine.

3.1.5 Specimen Production

For the Specimen Production, for each and every PLA filament it was used the printer 3D B2x300 provided by the company BEEVERYCREATIVE, represented in Figure 3.5.

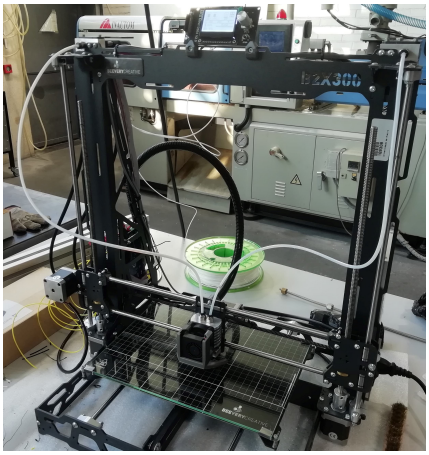

Figure 3.5: Beevery's 3D B2x300 3D printer.

The specimen was created in the software Solidworks, where its form and dimensions are determined from the sample type 5A described in the ISO 527-2:1996 norm [64], represented in Figure 3.6. The model was afterwards imported to the printing software 3D Ultimaker Cura. It was here that were defined all the printing parameters in accordance with previous works that studied the influence of the printing parameters on the mechanical properties [65]. The parameters were namely the the speed in which the printing process is done and the temperatures of both the extruder and the bed, specifically used for PLA. These parameters were revealed to be the most influential to the correct execution of the process as a whole. The specimen was printed in the centre of the bed, with the extruder and bed temperatures being 205°C and 60°C respectively. Table 3.1 summarises the printing parameters.

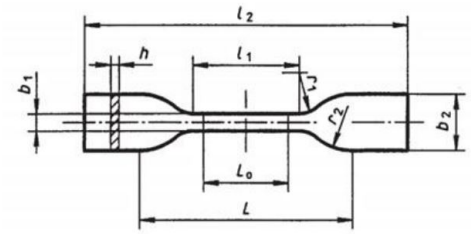

Dimensions in mm:

l_2	Total length, minimum:	≥75
b_2	End section width	12,5±1
l_1	Narrow section length	25±1
b_1	Narrow section width	4±1
r_1	Smaller radius	8±0,5
r_2	Bigger radius	12,5±1
L	Initial distance between grips	50±2
L_0	Measuring length	20±0,5
h	Thickness	≥2

Figure 3.6: Specimen design in accordance with the ISO 527-2:1996 norm.

Table 3.1: PLA printing parameters according to [65].

Parameters	**Values**	**Unit**
Part orientation	30	°
Printing angle	0	°
Layer thickness	0.1	mm
Extrusion width	0.4	mm
Interior fill	100	%
Printing Speed	60	mm/s
Extrusion temperature	205	°C
Bed temperature	60	°C

In the production of the specimens, there were no reported cases of problems regarding bed adhesion. After every impression, the specimen was laid until the bed temperature reached 50°C, being subjected to natural cooling, in view of preventing any strain created by its premature removal from the bed. All of the PLA specimens are shown in Figure 3.7.

Figure 3.7: 3D printed PLA specimens, from left to right: cPLA, vPLA and rPLA.

3.2 Adding Carbon NanoTubes

In the second major phase of this work, it was used MWCNTs as the mixing material with the vPLA and rPLA, having a density of 2.16 g·cm^{-3}, diameters between 20 and 40 nm and a length in the range of 1 μm and 2 μm. For this purpose, it was conducted a melting mixture or melt blending between both materials. Following this process, the

line of work is identical to the previous subsection, where the newly mixtured material will be submitted to the same three production phases previously mentioned.

3.2.1 Melt Mixing Materials

The melt mixing process was conducted using a Brabender Plastograph EC with a capacity of 20 m^3, shown in figure 3.8. As described in various literature articles, for the mixture to be done correctly, the humidity level present in the materials must be removed. To accomplish that, the PLA grains were dried at 50°C for 3 hours and the carbon nanotube particles were dried using the lyophilization equipment Telstar LyoQuest in Figure 3.8 for 24 hours before entering the mixing chamber.

(a)

(b)

Figure 3.8: (a) Brabender's Plastograph EC mixing machine, (b) Telstar's LyoQuest lyophilization machine.

The relative amounts of both materials were defined in Table 3.2, with carbon nanotubes content set in three different weight percentages. The mass of PLA used was 24 g when in conjunction with the higher percentage of nanotubes the volume occupied is 19.2 cm^3, remaining below the maximum capacity with a small margin to avoid and overfill.

Table 3.2: Relative wt% amount of the materials for mixture.

Mixture	**Content in wt%**	**Designation**
vPLA with MWCNT	0.5%	NvPLA0.5%
	1.0%	NvPLA1.0%
	1.5%	NvPLA1.5%
rPLA with MWCNT	0.5%	NrPLA0.5%
	1.0%	NrPLA1.0%
	1.5%	NrPLA1.5%

Concerning the temperatures used, after reviewing the literature, typical processing conditions correspond to temperatures between 160°C and 180°C [66; 67; 68], How-

ever,after analysing the DSC graphic, it can be concluded that the best range of temperatures to be used with this specific material is around the 180°C mark, being the one used with vPLA, while for the rPLA it was the temperature of 190°C the one used. As mentioned in the previous DSC subsection, when comparing both samples' analysis, it is noted that the rPLA one reaches the melting phase at a higher temperature than the vPLA sample, translating the necessity of a higher temperature input while still remaining within the range of the 180°C mark. The procedure when operating the mixer diverts from one sample to the other due to their macro nature. Having the benchmark of the mixing time shown in the literature to be around 10 minutes [69; 70], when mixing the vPLA, the input parameters used were 11 minutes at 180°C, whereas with the rPLA were 15 minutes at 190°C. While inserting the vPLA grains into the mixing chamber, it was registered a certain flow of the grains when getting into contact with the insertion wall and mixing blades, allowing the process to be done within 1 minute. However, a different approach was given when working with the rPLA, as this material, while getting into contact with any of the surfaces, tends to get viscous, forming a barrier which results in an obstruction to the mixing chamber. Even using a steel weight to force the insertion of the grains, this procedure takes longer than the vPLA one, being fully inserted after approximately 5 minutes.

As for the following procedures, it was the same as for the non mixed PLA materials described in the previous sections. However, during the filament production phase, despite using certain temperatures for the original materials, for the new nano based PLA grains it was measured new extrusion temperatures in order to extract the resulting filament with minimal flaws, safeguarding its correct insertion into the 3D printer. As such, for both the nano based vPLA (NvPLA) and the nano based rPLA (NrPLA) the most adequate temperature was 165°C. All the resulting nano mixed PLA specimens are shown in Figure 3.9.

Figure 3.9: 3D printed nano PLA specimens, from top to bottom the NrPLA and NvPLA and from left to right the amounts 0.5%, 1.0% and 1.5%.

On a final note regarding procedures, the specimen production was adjusted to better suit both of the new nanocomposites. In [71], it was registered signs of nozzle wear and degradation where, upon prolonged printing, the brass nozzle was abraded both inside the nozzle as well as on the front surface where it touches the printed object. This occurrence may cause clogging of the extruder nozzle which can be a hindrance to the printing process. A new stainless steel nozzle was used to replace the previous brass one and to provide a new consistency level to the printed specimens. Another change was the printing parameters, as the extruding temperatures were changed to 215°C to compensate for the new nozzle used and the printing speed, which was reduced from 60 mm/s to 20 mm/s in an attempt to correct a skidding problem that was observed when the filament was being pulled by the gear and pulley. On a more observation basis, the first layer of some specimens had some flaws while the base layer was being deposited, fact that would also occur while the printing process was being conducted, as some middle surface layers got inconsistently deposited. This was more frequent on the NvPLA rather than the NrPLA, which can contribute to the possible difference in results between the two nanocomposites.

3.3 Tensile Tests

For the final major phase of this work, mechanical longitudinal tensile tests were conducted to all produced specimens using a 100 kN Shimadzu AG-FX universal tensile test machine represented in Figure 3.10, at a crosshead speed of 1mm/min.

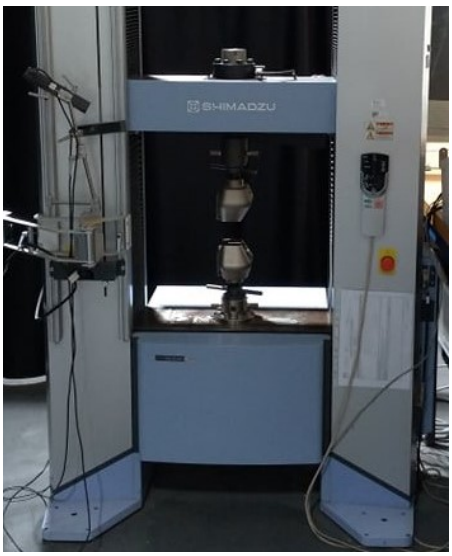

Figure 3.10: Shimadzu's 100 kN AD-FX universal tensile test machine.

The mechanical properties considered were the ones regarding the elastic behaviour of the specimen, since the application of the majority of AM components implies that they do not enter the plastic phase, or else risking a possible malfunction. These properties are the Young modulus (E) and the offset yield strength (σ_y), being this last one useful to define the approximate limit between the elastic behaviour and the beginning of the plastic one. Moreover, there can be isolated cases where plastic deformation is accepted,

meaning that the stress at break (σ_b) and strain at break (ϵ_b) might be useful to evaluate how much can the material endure before breaking, while defining a safe zone to operate it. Also, the ultimate strength (σ_u) of the material will be registered as well in order to determine how far the hardening phase will go before the occurrence of the necking. The parameters directly measured by the machine were Load (F) and length variation (ΔL). With these values, it was possible to obtain the stress, with Equation 3.1, and the strain, with Equations 3.2 and 3.3.

$$\sigma = \frac{F}{A_0} \quad \left[\mathrm{N} \cdot \mathrm{mm}^{-2}\right] \tag{3.1}$$

$$\epsilon = \frac{\Delta L}{L_0} \tag{3.2}$$

$$\epsilon = \frac{\Delta L}{L_0} \times 100 \quad [\%] \tag{3.3}$$

A_0 is the initial narrow section area and L is the initial distance between grips. The tensile yield strength was determined as the intersection of a straight line with slope equal to the modulus of elasticity, but with a strain offset of 0.2%, with the stress-strain curve. The ultimate strength and the stress and strain were also directly registered from the curve. The modulus of elasticity was calculated using the equation 3.4,

$$E = \frac{\sigma_2 - \sigma_1}{\epsilon_2 - \epsilon_1} \quad [\mathrm{MPa}] \tag{3.4}$$

σ_1 is the stress value corresponding to a strain of ϵ_1=0.05% and σ_2 is the stress value when ϵ_2=0.25%. For the purposes of this work, only the test samples complied with the referred standard [38] and not the testing method itself, which relied on the distance between grips for the strain calculations instead of using an extensometer.

Chapter 4

Experimental Results and Discussion

In the present section it is shown the detailed results of the tensile tests executed at the end phase of this work. These results will give the information needed to evaluate the completion of the work objectives, which will be discussed in the results analysis section. This discussion will include not only the evaluation of the results, but also a deep insight on all the factors that may contribute to any eventual discrepancies on each graphic comparison and corresponding values as dictated in the previous section regarding the tensile tests. The content for this section will be displayed firstly by the graphical results of each type of PLA, followed by the parameters obtained and calculated from said graphics, and secondly with the corresponding discussion subsection. It will contain a close analysis regarding the breaking nature of the specimens, tendencies of each graphic and calculated parameters when compared to its corresponding counterpart, and an overview on all materials, with every pro and con to be in alignment with the work objectives. The discussion will also attempt to connect every aspect registered in the previous chapter, notably the external factors that may have had a say in the nature of the results.

4.1 Tensile Tests Results

This procedure was the key element to understand how the various specimens would react mechanically, as shown by the following graphics regarding each type of specimen: cPLA in Figure 4.1, vPLA in Figure 4.2 with the corresponding NvPLA in Figure 4.3 to 4.5, and the rPLA in Figure 4.6 with the corresponding NrPLA in Figure 4.7 to Figure 4.9. The various general graphic results were paired with its corresponding elastic behaviour in order to correctly analyse the nature of the results, giving a better insight on the major differences between each type of PLA. Next, the parameters described in Section 4.2 were obtained with the information given by the result graphics and are shown in Table 4.1. They represent the average of the values registered with the corresponding standard deviations. These properties are also represented graphically in Figure 4.10 to visually compare each material's property. Every type of PLA was submitted to five tests, where the order of the tests were first the cPLA, followed by the vPLA and NvPLA, being completed with the rPLA and NrPLA.

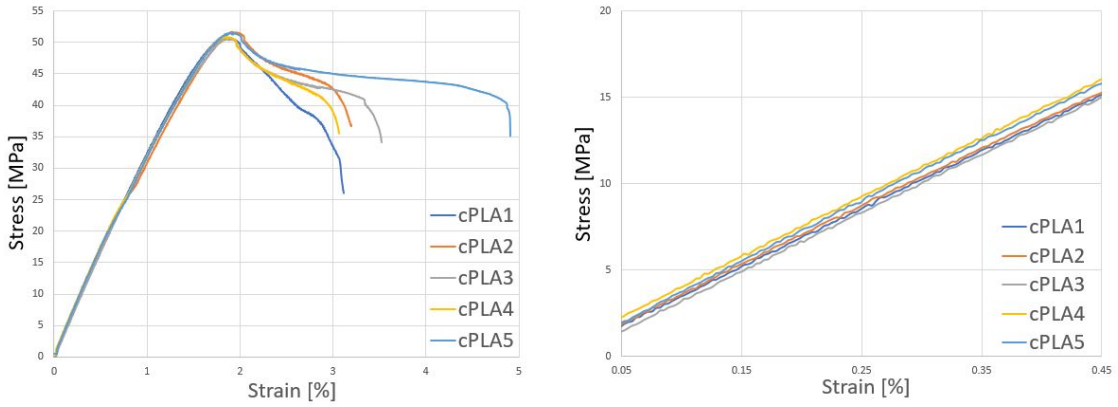

Figure 4.1: cPLA tensile test graphic results, from left to right: general graphic representing the full behaviour of the specimen, cPLA elastic behaviour within the 0.45% initial strain.

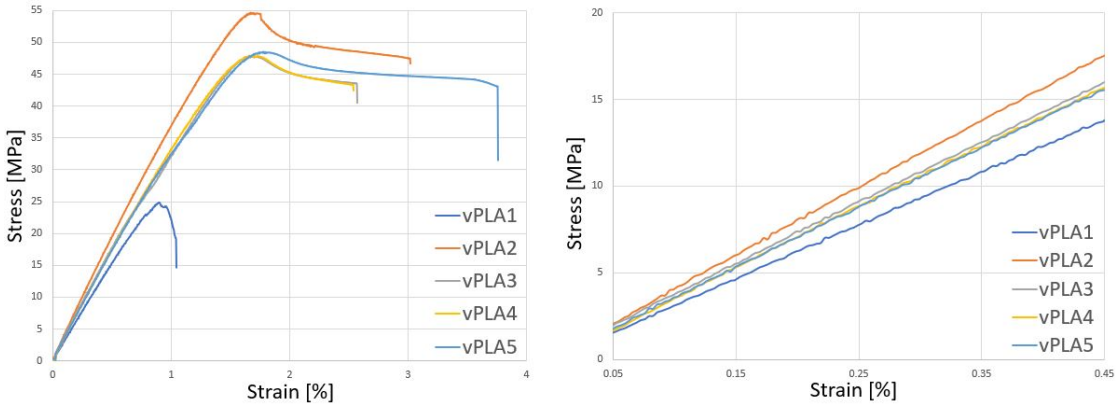

Figure 4.2: vPLA tensile test graphic results, from left to right: general graphic representing the full behaviour of the specimen, vPLA elastic behaviour within the 0.45% initial strain.

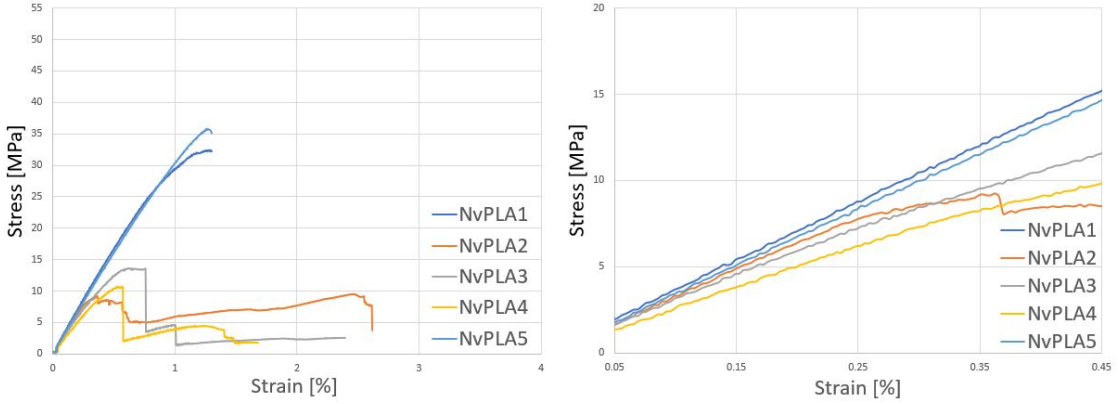

Figure 4.3: 0.5% NvPLA tensile test graphic results, from left to right: general graphic representing the full behaviour of the specimen, 0.5% NvPLA elastic behaviour within the 0.45% initial strain.

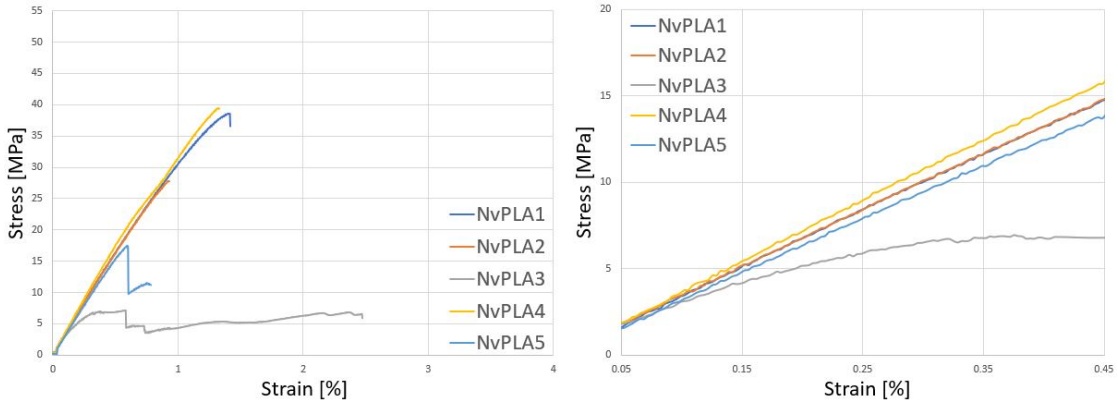

Figure 4.4: 1.0% NvPLA tensile test graphic results, from left to right: general graphic representing the full behaviour of the specimen, 1.0% NvPLA elastic behaviour within the 0.45% initial strain.

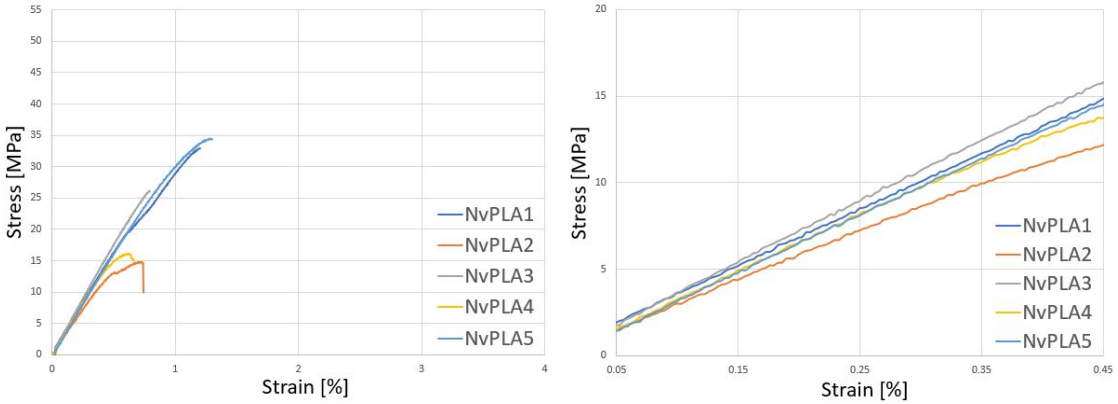

Figure 4.5: 1.5% NvPLA tensile test graphic results, from left to right: general graphic representing the full behaviour of the specimen, 1.5% NvPLA elastic behaviour within the 0.45% initial strain.

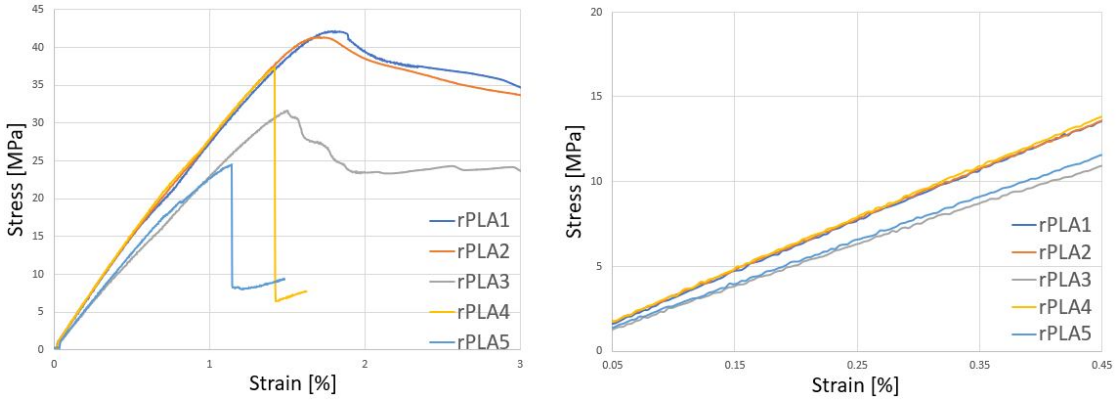

Figure 4.6: rPLA tensile test graphic results, from left to right: general graphic representing the full behaviour of the specimen, rPLA elastic behaviour within the 0.45% initial strain

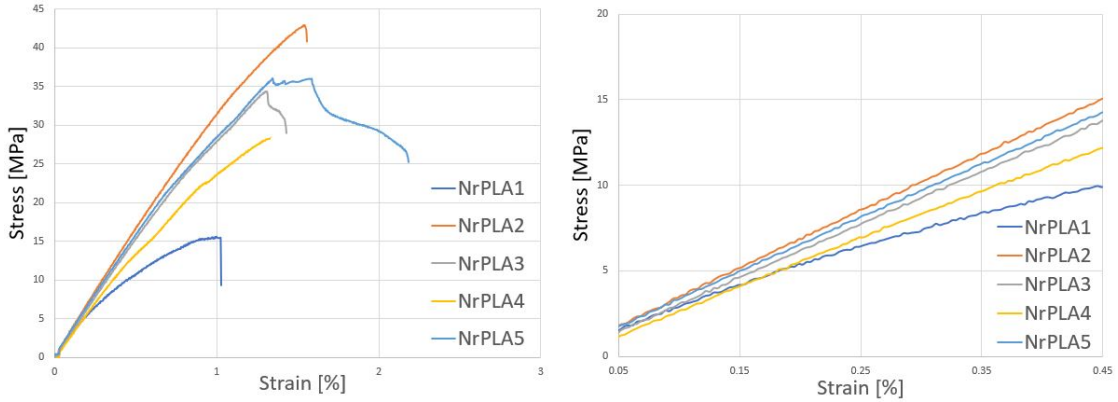

Figure 4.7: 0.5% NrPLA tensile test graphic results, from left to right: general graphic representing the full behaviour of the specimen, 0.5% NrPLA elastic behaviour within the 0.45% initial strain.

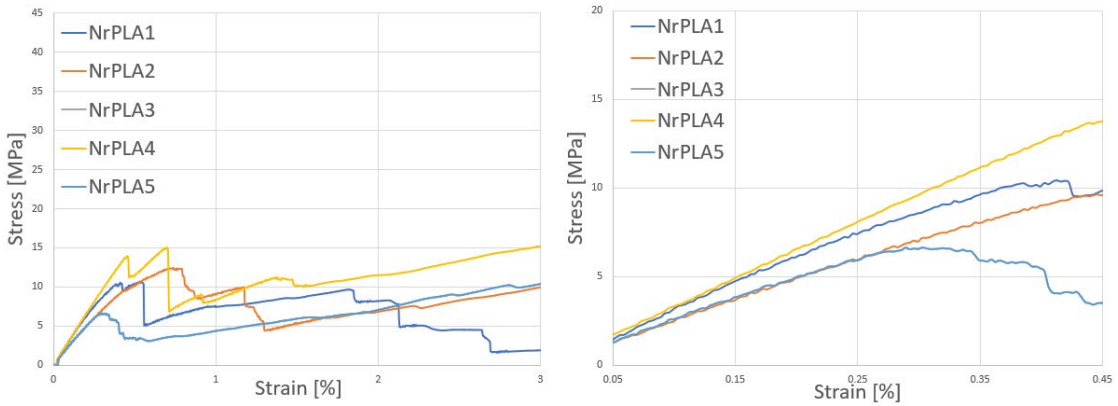

Figure 4.8: 1.0% NrPLA tensile test graphic results, from left to right: general graphic representing the full behaviour of the specimen, 1.0% NrPLA elastic behaviour within the 0.45% initial strain.

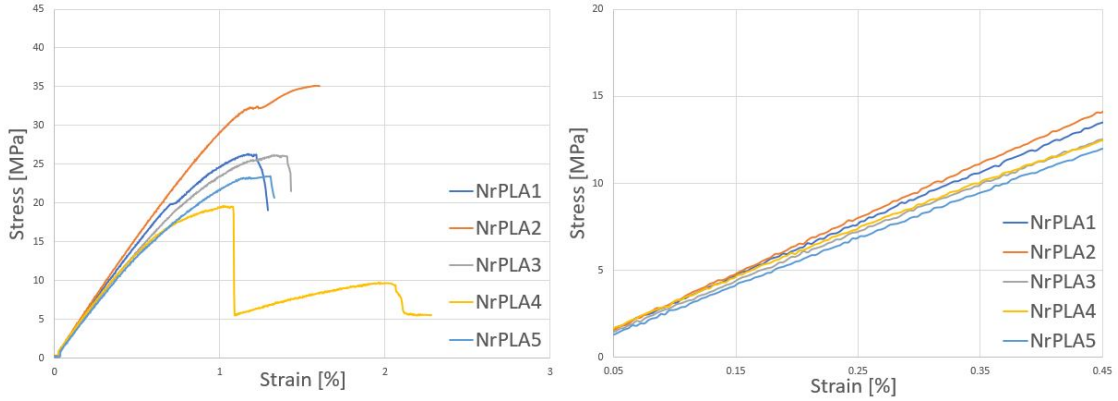

Figure 4.9: 1.5% NrPLA tensile test graphic results, from left to right: general graphic representing the full behaviour of the specimen, 1.5% NrPLA elastic behaviour within the 0.45% initial strain.

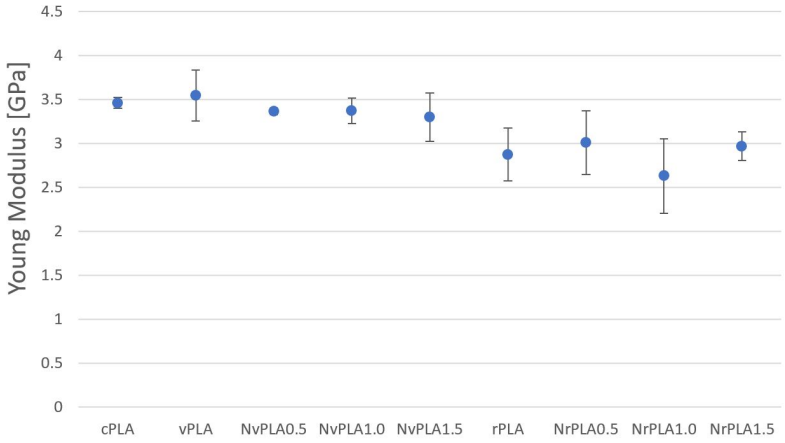

(a)

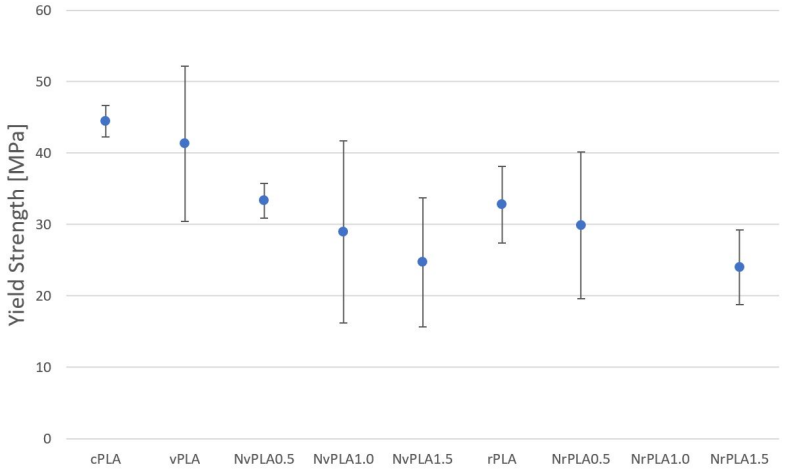

(b)

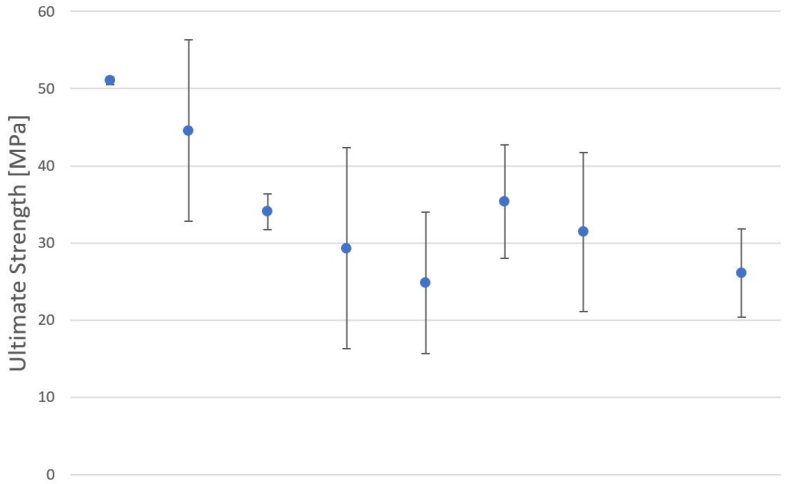

(c)

Figure 4.10: Parameters registered for each type of material with their corresponding standard deviation: (a) Young Modulus, (b) Yield Strength, (c) Ultimate Strength.

Table 4.1: Tensile Tests Parameters and corresponding standard deviation.

Specimen	$\boldsymbol{E}$ **[GPa]**	$\sigma_{\mathbf{y}}$ **[MPa]**	$\sigma_{\mathbf{u}}$ **[MPa]**
cPLA	3.46±0.06	44.48±2.21	51.02±0.46
vPLA	3.54±0.29	41.32±10.86	44.57±11.78
rPLA	2.87±0.30	32.78±5.38	35.36±7.35
NvPLA0.5%	3.36±0.03	33.35±2.44	34.06±2.32
NvPLA1.0%	3.37±0.14	28.99±12.74	29.30±13.02
NvPLA1.5%	3.30±0.28	24.71±9.04	24.83±9.19
NrPLA0.5%	3.01±0.36	29.90±10.28	31.43±10.32
NrPLA1.0%	2.63±0.42	Not Defined	Not Defined
NrPLA1.5%	2.97±0.16	24.05±5.23	26.13±5.70

Comparing the average values of the mechanical properties will bring forth a method of analysing each material, especially each counterpart and the corresponding evolution. Nevertheless, specific test results will be taken into account, especially regarding the yield and ultimate strength, to point out any potential in the nano mixed material or to highlight certain aspects found in that precise specimen, as there are cases where one test is heavily masked by the average value. Important to note that, due to the nature of the results, the stress and strain at break were not considered, as they deviate greatly from one to another. As such, for the discussion, it will only be considered the results regarding the elastic behaviour of the material through to its ultimate strength as a basis for comparison between the two types of PLA and their corresponding nano PLA counterpart. As said previously, more important than the plastic behaviour, is the elastic one where all the emphasis will be put into. In each right side graphic it is represented the zone which was used as a basis to calculate the Young Modulus, set within the range of 0.05% and 0.45%. Important to note that, as said in Section 4.2, this value is calculated in the interval ranging from 0.05% to 0.25%. However, to show more clearly the curve tendency in the elastic zone, an increase of 0.2% was set, visualising better the differences between each test and the discrepancy between one and another. Furthermore, for integral comparison purposes, the results registered in the table for the ultimate strength and yield strength are the ones related to the more accurate results, the ones who depict the real behaviour of the material not breaking prematurely. To set a limit for the selection criteria, for the average values it will not be considered those with an ultimate strength of 15 MPa or lower, as these were caused by a yielding phenomenon which will be explained afterwards in the next section.

4.2 Analysis and Discussion

After obtaining the results and corresponding graphics for each type of PLA, a handful of data can be acquired. On the cPLA graphic, it can be registered a tendency in the mechanical behaviour of all five tests, as they have extremely identical elastic region, confirmed by the low standard deviation, ending up reaching an ultimate strength of around 51 MPa. After reaching the ultimate strength they show several plastic tendencies, possibly meaning differences in the outcome of the printing process. From here onward, the cPLA results will not be considered as pivotal to elaborate conclusions regarding the evolution of the specimens, as they only represent the nature of the material

fabricated by its company.

Moving on to the next graphics, the vPLA shows a degree of consistency in three tests, being the vPLA2 test the one with the best result and the vPLA1 the worst. Being similar with the cPLA in regard to the plastic region, the vPLA reveals an ever so slightly better Young Modulus, ending up achieving the Ultimate Strength with less strain, despite the average values being lower. Analysing and comparing the standard deviation for the yield and the ultimate strength, it is revealed this inconsistent reaction, as their values are quite superior to the ones of the cPLA. Comparing now between the vPLA and the NvPLA, the results of the latter for all the three mixtures were distant from the former. Having registered the same problem of the vPLA1 on every nano test, the assumed more accurate results differ greatly from the vPLA in every parameter, not being able to reach the same values. Making a numerical comparison between both, it was registered discrepancies ranging from 23% to 44% of ultimate strength loss between the three mixtures. The Young Modulus was the parameter with the less drop, despite still ranging around the 5% and 6% loss. The complete discrepancies are represented in Table 4.2.

Table 4.2: Difference of the mechanical properties Young Modulus, Yield Strength and Ultimate Strength after mixing the vPLA with the MWCNTs

Comparison	**Young Modulus**	**Yield Strength**	**Ultimate Strength**
vPLA with NvPLA0.5%	-5.12%	-19.29%	-23.57%
vPLA with NvPLA1.0%	-4.92%	-29.85%	-34.26%
vPLA with NvPLA1.5%	-6.88%	-40.20%	-44.27%

These discrepancies highlight the worse quality of the MWCNT based specimens in comparison with its counterpart PLA material. Despite registering these values, it is important to mention the non existence of a plastic region in any of the better measured results. This shows the direct influence of the MWCNT, despite not reaching the same mechanical properties as the vPLA.

Regarding the rPLA, three different results are present. The rPLA1 and rPLA2 show identical plastic behaviour as the cPLA, not achieving the same Ultimate Strength and having lower Young Modulus. As for the remaining three, the rPLA4 and rPLA5 show a more fragile behaviour when compared with the previous two, with the former breaking much later than the latter. Initially the specimens behave as expected, however, after reaching a certain point, the specimens break in the same fashion as the vPLA1 and some of the NvPLA. The rPLA3 represents the same failure albeit with a different behaviour. What is strange, and interesting nevertheless, is the presence of two types of behaviour within the same material, revealing the tendency to have predominant plastic nature. Observing and comparing with the NrPLA, apart from the 1.0% NvPLA which features failures on all the five tests, it can be noted a change in nature, as more tests feature a now much less plastic behaviour. Only the 0.5% NrPLA shows a small plastic region, hinting that the quantity of MWCNTs was not enough to eliminate this plastic tendency, an aspect which was not seen heavily with the higher mixtures. Important to mention that there is an improvement of the Young Modulus when comparing the rPLA with the 0.5% NrPLA2 and 1.5% NrPLA2 tests, and a higher Ultimate Strength in the case of the 0.5% NrPLA2. Making a numerical comparison between both counterparts except for the 1.0% NrPLA, unlike the vPLA tests, there was an improvement of the Young Modulus

of around 4%. This will be the only positive as the other two properties registered a decrease, being more abrupt with the 1.5% NrPLA. The complete discrepancies are represented in Table 4.3.

Table 4.3: Evolution of the mechanical properties Young Modulus, Yield Strength and Ultimate Strength after mixing the rPLA with the MWCNTs

Comparison	**Young Modulus**	**Yield Strength**	**Ultimate Strength**
rPLA with NrPLA0.5%	4.73%	-8.78%	-11.13%
rPLA with NrPLA1.0%	-8.42%	Not Defined	Not Defined
rPLA with NrPLA1.5%	3.32%	-26.64%	-26.12%

These improvements regarding the Young Modulus show how the MWCNTs managed to improve the elastic nature of the rPLA, which showed to have a higher plastic tendency. Although not being able to correct all the turbulent plastic behaviour, it is a good indication of what can be done with a higher quantity of the additive material, which will be discussed later on. An interesting mention, looking more specifically at the 1.5% NrPLA2 graphic it represents an actual prediction of a standard tensile test, as it depicts the elastic zone and a quite visible Yield Point before initiating the Strain Hardening phase, breaking at the Ultimate Strength.

Leaving the general graphic results by, firstly it is important to understand one of the most key feature of all the tensile tests named the Wall Layer Fracture (WLF). This unfamiliar breaking phenomenon appeared in every test apart from the cPLA ones, occurring first during the vPLA1 test. After examining the broken specimen, this incident was certainly caused by the lack of adhesion between the grip section and the wall layers of the shoulder section, hence the name WLF. Afterwards, the specimen loses strength and rips apart, having the possibility of having two types of reaction, a brittle and a plastic one. Starting off with the vPLA, it was shown to be very brittle, as the specimen yielded in the shoulder area, breaking the link to the measuring length. In figure 4.11 (a), represented in pair with its corresponding tensile graphic figure 4.11 (b), is illustrated the brittle fracture behaviour of the vPLA. Highlighted in black amongst the other vPLA tests in grey, it represents graphically the observed mechanical failure. As the other four tend to their more natural behaviour, this one demonstrates a weak link in the described critical zone of the specimen, making it yield much earlier than it was supposed to. Checking visually the graphic, it also shows the lowest Young Modulus of the five present, possibly revealing its susceptibility to an early break.

Similarly, the rPLA shows an identical type of WLF albeit with a more prominent plastic behaviour. In this case, the specimen did not yield instantaneously in the shoulder zone, as it progressively cut open through the measuring length. In figure 4.12 (a) represented in pair with its corresponding tensile graphic figure 4.12 (b), is illustrated the plastic fracture behaviour of the rPLA. Also highlighted in black amongst the other vPLA tests in grey, it represents graphically the plastic rupture phenomenon. As time progressed, there were specific points were the specimen yielded in the critical zone and stretched. After every depression point, there might of been somewhat of a stress relief, which explains the tendency for the stress to increase despite the continuous increase in strain until it reaches a new depression point. As this goes on, the plastic region will continuously decrease until it finally breaks.

Approaching now the nano based PLA specimens, the WLF was identified as well, as

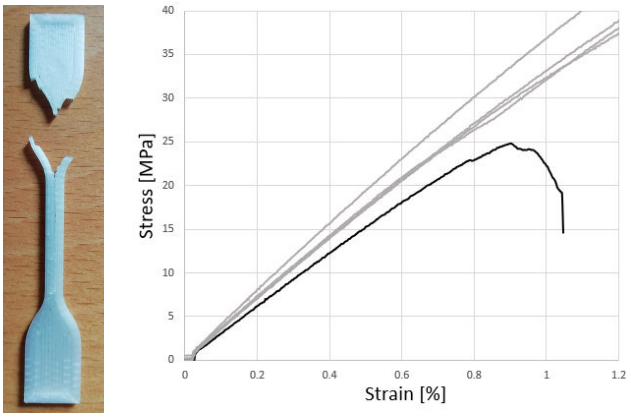

(a) (b)

Figure 4.11: Wall Layer Fracture with a brittle response: (a) state of the vPLA specimen after suffering the WLF, (b) corresponding tensile curve in black.

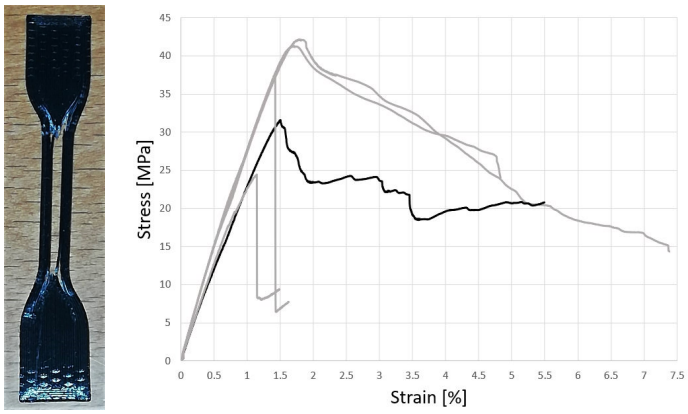

(a) (b)

Figure 4.12: Wall Layer Fracture with a plastic response: (a) state of the rPLA specimen after suffering the WLF, (b) corresponding tensile curve in black.

they were more recurrent on the NvPLA rather than the NrPLA ones, with the former having a somewhat different characteristic compared with the latter. As described in Section 4.2, changes to the printing parameters were made to ensure that the specimen was printed correctly. These changes were in order due to said nature of the NvPLA, as, even before the printing phase, the filament of both materials were distinct. The NvPLA filament was shown to be very brittle, while the NrPLA one was more plastic. This type of nature was somewhat altered during the printing process, as both the NvPLA and NrPLA showed tendencies of brittle behaviour and plastic tearing in the tensile tests. Nevertheless, the NrPLA still managed to have more plastic tendency. Figures 4.13 and 4.14 highlight said cases revealing for both materials the two types of breaking phenomenons, always paired with the respective graphic.

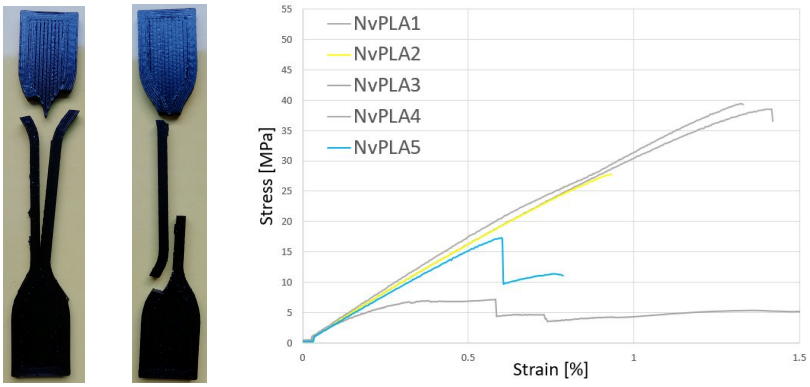

(a) (b) (c)

Figure 4.13: The yielding phenomenon on the NvPLA specimens: (a) NvPLA plastic break, (b) NvPLA brittle break, (c) corresponding graphic in blue and yellow respectively.

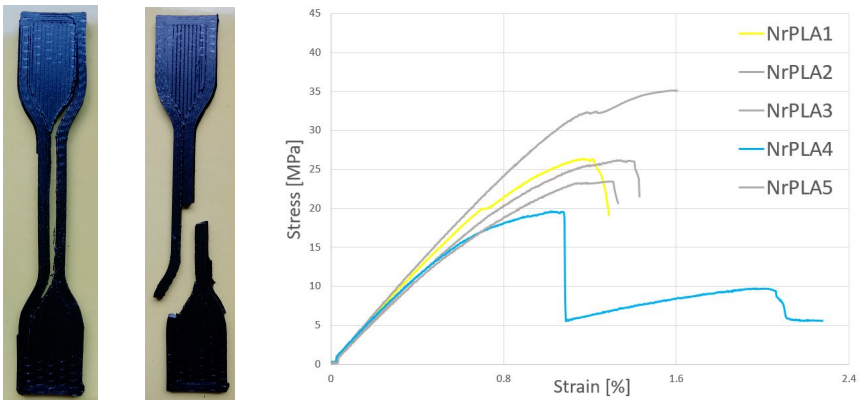

(a) (b) (c)

Figure 4.14: The yielding phenomenon on the NrPLA specimens: (a) NrPLA plastic break, (b) NrPLA brittle break, (c) corresponding graphic in blue and yellow respectively.

This unfamiliar breaking phenomenon was soon diagnosed as caused by the ap-

proach used when modelling the specimen on Ultimaker Cura, which is represented in Figure 4.15. With the intention of making the layers of the specimen as straight as possible and with a coherent structure in view of the tensile tests, it was added wall layers to ensure these objectives. However, observing how the tests panned out, it demonstrated to not be the most adequate approach, as a handful of information might not have been spotted due to their nature, as explained next.

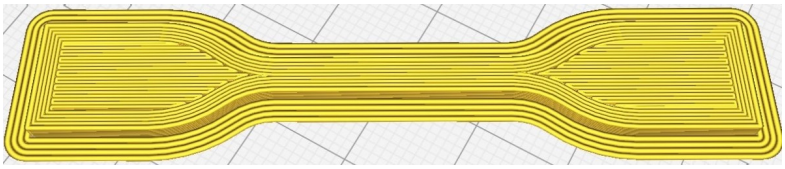

Figure 4.15: Layer definition of the specimen on Ultimaker Cura

With respect to the quality of the specimens, the graphics that can give some insight on how the nano mixtures should correctly behave are the ones that did not yield early due to the WLF and open through the gauge length, managing to continue to accumulate stress despite the progressively increase in strain. Examples of this are shown for instance in figure 4.2 (b) represented by the NvPLA1 and NvPLA5. In the end, despite having different outcomes in terms of results, the specimens will break the same way in one of the sides of the wall layer, whether it be in the measuring length or in the shoulder. Regarding the specimens' behaviour more specifically, the curve representation resembles that of a ceramic material, as the lack or non existence of a plastic region reveals evidently its fragile nature. The other key feature of this graphic is its Ultimate Strength before the rupture, being much lower to the ones registered with the non mixed PLA materials, being the only exception the 0.5% NrPLA2 test. There is a possibility that the newly formed composite has a worse quality of material, which in any case as to be diagnosed. The mixture of virgin material with MWCNT in the terms established in this work may not suffice to produce reliable specimens to use as a solid basis of comparison. Another possibility is the contamination and quality of mixing, which both will be analysed afterwards. Nevertheless, when pairing each type of PLA with its corresponding nano mixed PLA, it is possible to analyse that the NrPLA is the one that closes the gap more to its counterpart in terms of the value of the Ultimate Strength and Young Modulus. The recycled material, having been through certain processes and possibly being injected with additives of an unknown nature, might contain the certain characteristics that can ease the mixture and still boost its performance. Although this possibility exists, the contrary can also occur where the recycled material, after enduring various types of strain after its usage, can hinder any attempt at mixing with other materials, especially with a nanomaterial, as some tests still contain a plastic region defined albeit short, such as the 0.5% NrPLA5 or 1.5% NrPLA5.

One more aspect that requires discussion is the nature of the assumed more accurate results, the ones which, despite breaking in the same fashion as the worst specimens, still managed to accumulate a moderate level of stress before breaking. The basis for this topic is the difficult task of measuring the yield strength. As some of the results indicated, there were specimens that showed the elastic region ending abruptly, in comparison with other specimens of the same mixture, possibly still due to the occurrence of the WLF. Seeking the 0.2% offset strain value to determine the yield strength was not possible to

the already mentioned abrupt end. As seen in figure 4.2 (c) for the NvPLA2 test and (d) for the NvPLA3, the offset graphic could not intersect with the tensile curve. In some tests, the yield strength region could be estimated to be an ever so slightly decrease of the steep level of the corresponding ephemeral elastic part of the tensile curve. While this proved to be a difficult task to accomplish, in another handful of curves there was practically no presence of such decrease in steepness, translating in the impossibility of acquiring the yield strength. In these cases, it is assumed that the yield strength is equivalent to the Ultimate Strength, once again being similar to that of a ceramic material. However, this assumption might not be accurate and might not represent what truly happens in reality. Combining this with the WLF, there is no guarantee that the end of the elastic zone for the specific material is when the specimen breaks, as the WLF prevents one from diagnosing the true nature of the material. Another factor that verifies this hypothesis is present in figure 4.2 (c), as the NvPLA2 follows the same tendency as the NvPLA1 and NvPLA4 with approximately the same Young Modulus, when, suddenly, it breaks earlier. Having identical elastic behaviour until the rupture and the possibility of occurring the WLF, the NvPLA2 should at least reach the same height as the other two. Likewise, the same two might even still be able to reach further, as the wall layer yielding prevents from drawing any more conclusions.

The original benchmark used for the analysis of this work was an increase of a minimum of 5% of the values for the original non mixed specimens as an improvement to the mechanical properties and a reduction of the plastic zone. Getting together all the assumed more correct results and removing the specimens prematurely affected by the WLF, it is confirmed the almost complete reduction to zero of the plastic zone. In terms of the properties, as mentioned before, only the NrPLA got an improvement in terms of the Young Modulus when compared to its counterpart. However, this evolution was cut short to the 5% mark, not reaching the objective set. Analysing the elastic region as a whole, the results of the pair stress and strain are low compared to expectations which took for granted that the specimen would have its elastic zone extended a little further. Figures 4.16 and 4.17 shows the overlap between the non mixed and the nano mixed materials, giving a visual way to observe this discrepancy. Important to note that the 1.0% NrPLA is not represented as all the specimens belonging to this group suffered the WLF as shown in figure 4.8.

As for the specific values, the benchmark was obviously not reached, with the exception of the 0.5% NrPLA2 test. In this sole trial, it was shown the potential of the application of the nano tubes in the plastic. The only downfall is that a single trial should not determine the general conclusion of this work, as more results like this one should have been obtained. Throughout all the experimental phases there were factors that might have influenced or in a way contributed to the nature of these results.

Starting off with the drying phase, the applied conditions of lyophilisation can impact the stabilisation of nanomaterials during and after freeze-drying, especially the velocity of freezing, the pressure and temperature, and the duration of each stage of the process. Working with MWCNTs may or may not be as critical, but with the newly formed PLA nanocomposite, the normal drying process can disrupt the dispersion of the nanomaterial in the PLA matrix. In these conditions, there is a possibility that the extrusion phase might not go as smoothly. After the melt blending process, the resulting material might not have had the best mixing shape, as there is a possibility both PLA and the Carbon Nano Tubes got wrongly mixed. Also the amount of nano material used might not be

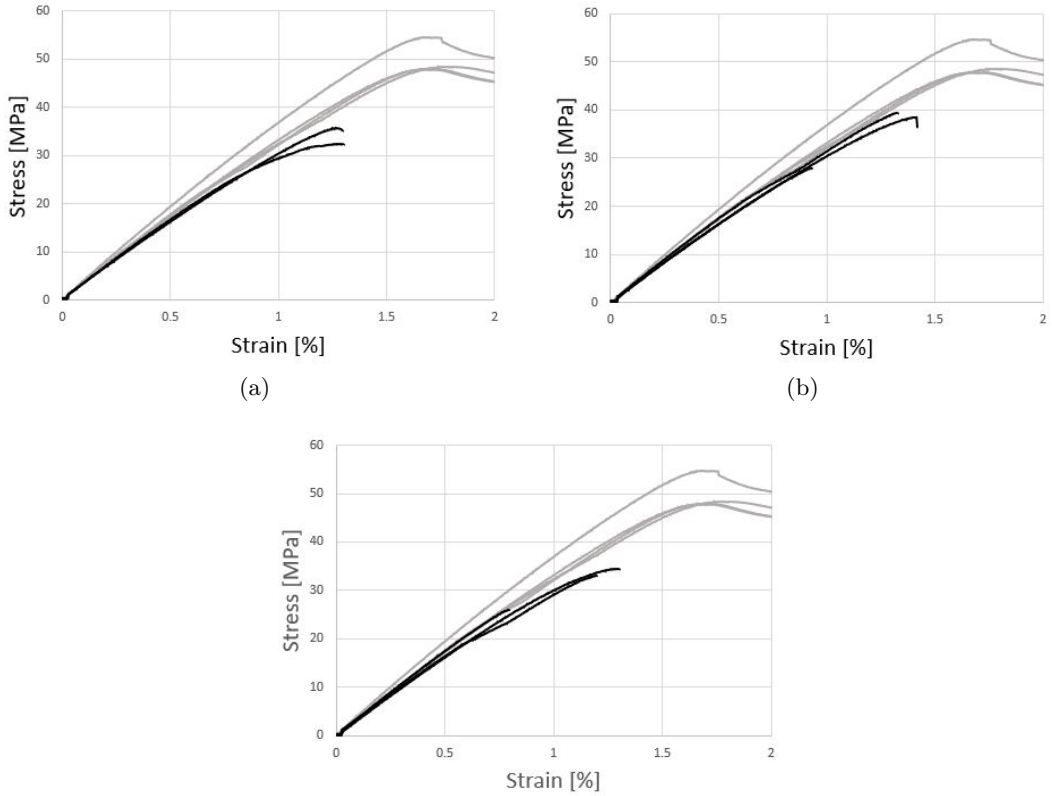

Figure 4.16: Visual overlap of the vPLA in grey with the NvPLA counterpart in black: (a) vPLA with the 0.5% NvPLA, (b) vPLA with the 1.0% NvPLA, (c) vPLA with the 1.5% NvPLA.

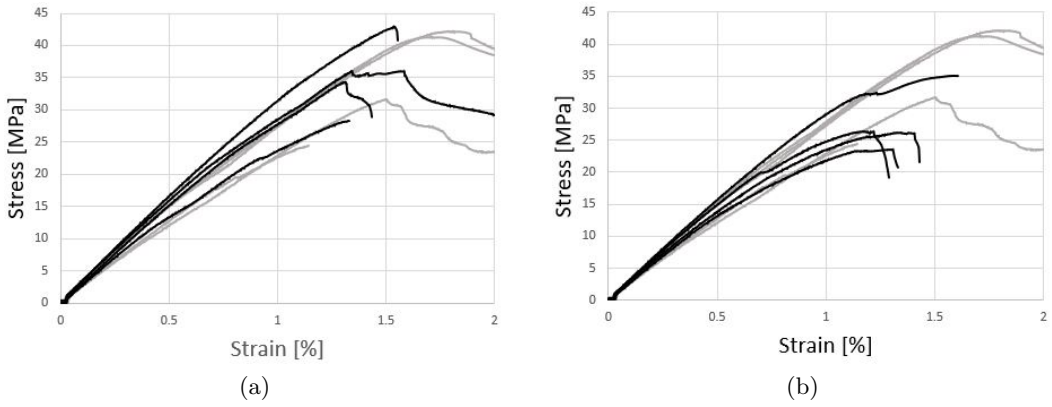

Figure 4.17: Visual overlap of the rPLA in grey with the NrPLA counterpart in black: (a) rPLA with the 0.5% NrPLA, (b) rPLA with the 1.0% NrPLA, (c) rPLA with the 1.5% NrPLA.

enough to give the newly formed plastic an integral structure, one that especially avoids the WLF problem or any rupture involving the wall layers. Another possibility was the lack of quality of the grains or the produced filament. After the mixture, the resulting crushed grains had somewhat of an unknown nature, making it difficult to reach the best extrusion temperature range. The temperature set was based on the filament's shape while being extruded, as the best one was set in view of the straightness of the filament in order to be set correctly in the printer. However there was no guarantee that it was optimal temperature in terms of the quality itself.

The contamination passed from a previous material to the next one being used in a certain process is also to be heavily considered. This happened more notoriously in the filament extrusion phase, where the risk of contamination is moderate to high. Despite taking place a cleaning process to avoid said fact, this action may be imperfect and it will not suffice, as there would still be traces of a previous material left inside. In conjunction with every mixed sample successively inserted into the equipment, the degree of error might scale further. Another factor that can alter the nature of the results is the non guaranteed uniformity of the content throughout the length of the filament, and may well occur in conjunction with the contamination problem. The entrance to the extrusion chamber through the never ending screw can occasionally get clogged due to the over dimension of the grains, disturbing the steady flow of grains momentarily. Although it is easy to correct this occurrence by forcing the grains' entrance, it is always important to note and consider it a possible factor that can alter the quality of the filament per length.

Another source of possible contamination might be while undergoing the melt mixing phase. The plastic extraction process is not ideal, being also dubious when it comes to safeguarding the correct concentration levels of MWCNTs, let alone the presence of random impurities related to not having a perfect cleaning process or traces of dust and other wastes that have settled between days of work. Once again, the successive mixtures taken place in the equipment will likely result in an amass of the concentrations levels of the MWCNTs.

Deviating from this, another factor that might influence the correct extraction of filament is the degree of dryness of the grains. As described in its corresponding section, the state of the filament must be observed empirically, more importantly its state of roughness. Having the filament a certain degree of roughness, it may indicate the presence of a small percentages of humidity, which can be a hindrance to the quality of the resulting printed specimen. One element that can disturb the degree of humidity is the possible occurrence of chunks of air flow, as the grain storage chamber is not entirely sealed.

In the final experimental phase, the specimen production using the printer, there were problems reported regarding the extruder nozzle, where occurrences of clogging were registered. This hampered the normal flow of the experiments, as a cleaning process had to take place after each type of filament used. While the printing was being done, it was also frequent the occurrence of a blockage in the extrusion chamber, caused by the shattering of the filament inside. This would temporally halt the process, as a small pause had to take place. This temporary setback could affect the normal flow of the procedure, making it a factor to be taken into account.

Chapter 5

Final Remarks

5.1 Conclusions

Having as a basis the content from the analysis and discussion subsection, there are some important ideas that become clear. Enhancing both the material produced and its application is an important aspect in view of this work, always to be considered. Upgrading the resulting components will always be of an interest to any company producing with 3D printers and even to the common user, as they can utilise certain parts needed for a specific role without having the need to invest abundantly.

Having said this, overall this work demonstrated the difficulty in analysing and applying such types of enhancements, especially at the nano level. Work conditions demonstrated to be pivotal to accomplish the desired results. Working in a delicate context, such as using nanomaterials, requires a certain degree of precision, which is fundamental to correctly evaluate the nature of the results. This degree would also come with a level of supervision after each step of the work, to ensure and safeguard the correct and equal manipulation of all the materials involved. All these aspects would be necessary to employ a viable general process which can be used later in other applications. However, despite almost securing consistent results, in terms of their quality there are other points of improvement needed. Viability with MWCNTs requires their use in a higher percentage, or at least at an higher difference between each amount, especially when working with two types of plastic that show to be very distinct. Hence the need of a more accurate use of the MWCNTs to amplify their elastic potential while, at the same time, reducing their plastic behaviour. While mentioning the plastics used, the importance of knowing every detail in their background is essential to create a predictive model regarding the reactions they may show after getting into mixtures. The vPLA was somewhat informative regarding its properties and origins, whereas the rPLA remained an unknown factor throughout the whole work. Not knowing properties such as its density, or past uses before being recycled or even any kind of additives that this material might have gotten, constituted as a barrier to correctly predict how to process the material and adjusting it to the optimal parameters of use. This aspect regarding additives would be with respect to how many times this material was recycled, being important in regard to the mixing behaviour with the nano tubes.

Moving on to arguably the most impactful outcome of this work, the Ultimaker Cura specimen model was ultimately revealed to be a key factor on the final results. The way it was designed sentenced how the specimens would behave when submitted to the tensile

tests, an occurrence only diagnosed during said tests, thus being unable to be reverted. The WLF was critical in influencing the outcome of the majority of the tensile tests which for one informs of the necessity of making the modelling more robust. Unlike the more common metal specimens, the integrity of plastic FDM ones, require special attention due, in majority, to the various layers that composed them and, especially, their alignment. Although the use of wall layers might not necessarily be wrong, their use in excess just to fulfil the required norm certainly is, and, as observed empirically and graphically, compromises the results. Nevertheless, the specimens that endured such mechanical failure showed promise in terms of elastic value gained from the nano mixture, but, as said previously, a change in the MWCNTs approach should be put into effect.

Overall, the work ended up being highly influenced by the specimen model and the quality of the melt blending process. Being the quality of the mixture unknown throughout all the experimental phase was somewhat of a silent factor waiting to be revealed during the most crucial phase of the work, including the printing phase. The WLF was shown to be critical, however, perhaps with a better insight into the quality of the mixture, said phenomenon could have been postponed to higher values of stress and strain, highlighting what should be a much more accurate result. Nevertheless, there were still positives aspects to be taken into account, such as the surprising smooth printing and extrusion operation of the nano based PLA, where much more difficulties were expected but not registered. Also, it is always important to note the results that showed more promise, despite not being able to reach the expected values. In conjunction, all these aspects combined can contribute for better results, having always in mind the integrity of the material and setting predictive models that can give the information needed to ensure to correct execution of all the work.

5.2 Future Work

Having previously set a basis for this work, it continued as a project of plastic reinforcement, which, as described in the majority of the sections, needs to be set in a specific environment, carefully picked materials and working parameters that suits the needs of said materials. As for what tomorrow brings, the list grows on the possibilities of work that can be done based on the results of this thesis and all of its inherent experimental work.

The first course of action would be to give more emphasis on every single specific work phase rather than the process as a whole. Studying and analysing all the plastic transformations throughout the work will provide an important insight on how the material is evolving, for better or worse, and will drive the next course of action based on the same analysis. Instead of doing a set plan A, there will be a possibility of refining the same plan to a more robust one, preventing typical errors from occurring. Having this work as a specific example, examining the safeguard of either the non mixed PLA and the mixed one, after each process it is important to run tests such as the DSC one to ensure that the user is setting the correct parameters to the next procedure. The importance grows as new materials arise such as the nano mixed ones, where its nature is relatively concealed until further analysis such as this scan. Studying the material's nature can be done, not only through the parameter of temperature, but with scanning

its structure, in this case more specifically the produced filament. Different types of PLA bring different mechanical behaviours as seen in the results section. Verifying the state of the filament, whether its brittle or flexible on a macro perspective or its post mixture ratio content through the radius on a micro perspective, might be of use in order to inform the user on how to proceed the work, adjusting the parameters deemed fit to obtain the required results. Lastly regarding the material's nature, it would be interesting to know and to create the story of the used plastic, more importantly any recycled material. One tough obstacle in the results discussion was the unknown nature of the rPLA, only having a small lead that it originated from previous operational parts. The process in which they were submitted and all possible additives that the plastic was injected are unknown, making it difficult to conclude anything with accuracy. As such, creating a recycled plastic where its past is known might be a good start to compare how much of a difference it makes when paired with the virgin plastic.

The same logic can be applied to the additive material, in this case the MWCNTs, where there are several routes that can be taken to, at least, try to correct some errors associated with the experimental phase of the nanomaterial. Starting with their drying process, freeze-drying of nanomaterials can be a very complex process that requires a careful delimitation of the process conditions. As such, just like the scanning of the material taken to each phase, a more careful drying process should be operated, in order to keep safeguarding the material. Another route while working with the MWCNTs is adjusting the mixing parameters and search for the optimal mixing conditions. As mentioned in the discussion phase, there were various factors that might have had an influence in determining the quality of the mixed material, however there is still the possibility of optimising the mixing environment, one aspect that should always be focused on.

On a second note, an interesting route which can be taken is to study how the tensile tests results vary when changing the printing model of the specimen. As noted in the results discussion section, the modelled specimens in which occurred the rupture throughout the measuring length due to the WLF, was shown to be critical to the integrity of the final results. Altering this approach to a more optimised one might help in obtaining more accurate tensile graphics and corresponding mechanical parameters of each type of material. Comparing each approach with its corresponding results would also give an interesting insight on the printing process itself, as refining the layer-by-layer can come with its set of advantages.

Another interesting route concerns the regulation of the tensile tests in regard to the speed used. Varying it and comparing each result would give insight to whether the tensile speed affects the resulting outcome of the specimens. More importantly, this change can be an interesting way of analysing if the WLF occurs with the same tendency as the one shown in this work. Another approach during the tensile tests is to check if the elastic region of the specimens stay true to what was determined by the offset value of the yield strength, by analysing, with an extensometer or another measurement tool, if the shape of the specimen returns to its original state. This can be useful in the sense that it might give a better definition of the elastic region, and in conjunction with lower speed values, might give an accurate representation of the pretended zone.

All these suggestions are intended to help correct all the negative aspects of this work, combining with the already known positives to ensure its correct execution. There will always be variables that prevent the user from proceeding smoothly throughout all

the experiments, being reduced in number as correction measures are implemented. This way, not only the quality of the results but also the time in which they are obtained, is optimised, leading to a much faster work phase without compromising said results and tarnishing the objectives established.

Bibliography

[1] American Society for Testing and Materials. *Standard Terminology for Additive Manufacturing Technologies*, pp. 1–3, 2013.

[2] ASTM Internationl, *Helping our world work better, The Global Leader in Additive Manufacturing Standards*, pp. 2, 2017.

[3] Jamie D., *3D Printing vs CNC Machining: Which is best for prototyping?*. Available in: https://www.3dnatives.com/en/3d-printing-vs-cnc-160320184/. (Accessed in 26/02/2019).

[4] C. Lindemann, U. Jahnke, M. Moi, R. Koch, Analyzing Product Lifecycle Costs for a Better Understanding of Cost Drivers in Additive Manufacturing, *Solid Freeform Fabrication Symposium - An Additive Manufacturing Conference*, Vol. 23, pp. 177-188, Austin, Texas, USA, 2012.

[5] N. Hopkinson, R.J.M. Hague, P.M. Dickens, *Rapid manufacturing, An industrial revolution for the digital age*, Edition: John Wiley, Chichester, England, 2006.

[6] S. Legutko, Additive techniques of manufacturing functional products from metal materials. *IOP Conference Series: Materials Science and Engineering*, Vol. 393 (1), 2018.

[7] BIBUS MENOS, drukarki3D.pt. *Ready Products*. Available in: https://drukarki3d.pl/zastosowania/gotowe-produkty/. (Accessed in: 01/03/2019).

[8] M. Javaid, A. Haleem, Additive manufacturing applications in medical cases: A literature based review. *Alexandria Journal of Medicine*, Vol. 54 (4), pp. 411–422, 2018.

[9] E. Winick, *Additive Manufacturing in the Aerospace Industry*. Available in: https://www.engineering.com/AdvancedManufacturing/ArticleID/14218/Additive-Manufacturing-in-the-Aerospace-Industry.aspx, 2017. (Accessed in: 05/03/2019)

[10] T. D. Ngo, A. Kashani, G. Imbalzano, K. T. Q. Nguyen, D. Hui, Additive manufacturing (3D printing): A review of materials, methods, applications and challenges, *Composites Part B: Engineering*, Vol. 143, pp. 172–196, 2018.

[11] K. Carlson, 3D printing adds another dimension as tool for production, not just prototypes, *The Seattle Times*. Available in: https://www.seattletimes.com/business/technology/

3d-printing-adds-another-dimension-as-tool-for-production-not-just-prototypes/. (Accessed in: 05/03/2019).

[12] L. Langnau, *A closer look at extrusion-based 3D printers*, *Make Parts Fast, A Design World Resource*. Available in: https://www.makepartsfast.com/a-closer-look-at-extrusion-based-3d-printers/. (Accessed in 05/03/2019).

[13] S. H. Ahn, M. Montero, D. Odell, S. Roundy, P. K. Wright, Anisotropic material properties of fused deposition modeling ABS. *Rapid Prototyping Journal*, Vol. 8 (4), pp. 248–257, 2002.

[14] B. Evans, *Practical 3D Printers: The Science and Art of 3D Printing*, Apress 1st edition., 2012.

[15] D. T. Pham, R. S. Gault, A comparison of rapid prototyping technologies. *International Journal of Machine Tools and Manufacture*, Vol. 38, pp. 1257–1287, 1998.

[16] Stratasys Inc., Fused deposition modelling for fast, safe plastic models, *12th Annual Conference on Computer Graphics*, Chicago, pp. 326–332, 1991.

[17] B. Huang, S. Singamneni, *Alternate slicing and deposition strategies for Fused Deposition Modelling*, PhD thesis, Auckland University of Technology, 2014.

[18] E. Verdonck, K. Schaap, L. C. Thomas, A discussion of the principles and applications of Modulated Temperature DSC (MTDSC). *International Journal of Pharmaceutics*, Vol. 192 (1), pp. 3–20, 1999.

[19] D. A. Skoog, F. J. Holler, S. R. Crouch, *Principles of Instrumental Analysis*, Thomson Brooks/Cole 6th edition, 2007.

[20] K. V. K. Kodre, S. R. S. Attarde, P. P. R. Yendhe, R. Y. R. Patil, V. V. U. Barge, Differential scanning calorimetry: a review, *Research and Reviews: Journal of Pharmaceutical Analysis*, Vol. 3 (3), pp. 11–22, 2014.

[21] I. B. Durowoju, K. S. Bhandal, J. Hu, B. Carpick, M. Kirkitadze, Differential scanning calorimetry — A method for assessing the thermal stability and conformation of protein antigen. *Journal of Visualized Experiments*, Vol. 2017 (121), pp. 1–8, 2017.

[22] L. D. B. Machado, ; J. R. Matos, *Técnicas de Caracterização de Polímeros*, 2003.

[23] S. Japar, M. S. Salit, The development and properties of biodegradable and sustainable polymers. *Journal of Polymer Materials*, Vol. 29 (1), pp. 153–165, 2012.

[24] Natureworks LLC, Technology Focus Report: Toughened PLA. Available online at: https://www.natureworksllc.com/~/media/Files/NatureWorks/Technical-Documents/White-Papers/Toughened-PLA-Technology-Focus-pdf.pdf.

[25] R. Auras, B. Harte, S. Selke, An overview of polylactides as packaging materials. *Macromolecular Bioscience*, Vol. 4 (9), pp. 835–864, 2014.

[26] D. J. Sawyer, Bioprocessing — no longer a field of dreams. *Macromolecular Symposia*, Vol. 201 (1), pp. 271–282, 2003.

[27] R. E. Drumright, P. R. Gruber, D. E. Henton, Polylactic acid technology. *Advanced Materials*, Vol 12 (23), pp. 1841–1846, 2000.

[28] J. R. Dorgan, H. J. Lehermeier, L. I. Palade, J. Cicero, Polylactides: properties and prospects of an environmentally benign plastic from renewable resources. *Macromolecular Symposia*, Vol. 175 (1), pp. 55–66, 2001.

[29] K. A. Athanasiou, G. G. Niederauer, C.M. Agrawal, Sterilization, toxicity, biocompatibility and clinical applications of polylactic acid/polyglycolic acid copolymers. *Biomaterials*, Vol. 17 (2), pp. 93–102, 1996.

[30] Y. Kimura, K. Shirotani, H. Yamane, T. Kitao, Ring-opening polymerization of 3(S)-[(benzyloxycarbonyl)methyl]-1,4-dioxane-2,5-dione: a new route to a poly(.alpha.-hydroxy acid) with pendant carboxyl groups. *Macromolecules*, Vol. 21, pp. 3338–3340, 1998.

[31] B. Eling, S. Gogolewski, A. J. Pennings, Biodegadable materials of poly(l-lactic acid): 1. Melt-spun and solution spun fibers. *Polymer*, Vol. 23 (11), pp. 1587–1593, 1982.

[32] E. T. H. Vink, K.R. Rábago, D. A. Glassner, P. R. Gruber, Applications of life cycle assessment to NatureWorks polylactide (PLA) production. *Polymer Degradation and Stability*, Vol. 80 (3), pp. 403–419, 2003.

[33] Y. Tokiwa, B.P. Calabia, Biodegradability and biodegradation ofpoly(lactide). *Applied Microbiology and Biotechnology*, Vol. 72(2), pp. 244–251, 2006.

[34] R. M. Rasal, D. E. Hirt, Toughness decrease of PLA–PHBHHx blend films upon surface-confined photopolymerization. *Journal of Biomedical Materials Research Part A*, Vol. 88 (4), pp. 1079–1086, 2009.

[35] M. Hiljanen-Vainio, P. Varpomaa, J. Seppälä, P. Törmälä, Modification of poly(L-lactides) by blending: Mechanical and hydrolytic behavior. *Macromolecular Chemistry and Physics*, Vol. 197 (4), pp. 1503–1523, 1996.

[36] A. V. Janorkar AV, Metters AT, D. E. Hirt, Modification of poly(lactic acid) films: enhanced wettability from surface-confined photografting and increased degradation rate due to an artifact of the photografting process, *Macromolecules*, Vol. 37 (24), pp. 9151-9159, 2004.

[37] B. D. Ratner, Surface modification of polymers: chemical, bio-logical and surface analytical challenges, *Biosensors and Bioelectronics*, Vol. 10, pp. 797–804, 1995.

[38] K. J. L. Burg, Jr W. D. Holder, C. R. Culberson, R. J. Beiler, K. G. Greene, A. B. Loebsack, et al, Parameters affecting cellular adhesion to polylactide films. *Journal of Biomaterials Science, Polymer Edition*, Vol. 10(2), pp. 147–161, 1999.

[39] ISO/TS 27687:2008(en), Nanotechnologies - Terminology and definitions for nanoobjects - Nanoparticle, nanofibre and nanoplate.

[40] S. Iijima, *Nature*, Vol. 354, pp. 56–58, London, 1991.

[41] S. C. Hong, S. Myung, Nanotube Electronics: A flexible approach to mobility. *Nature Nanotechnology*, Vol. 2 (4), pp. 207–208, 2007.

[42] R. Khare, S. Bose, Carbon Nanotube Based Composites A Review. *Journal of Minerals and Materials Characterization and Engineering*, Vol. 4 (1), pp. 31-46, 2005.

[43] P. J. F. Harris, Carbon nanotube composites. *International Materials Reviews*, Vol. 49 (1), 31–43, 2004.

[44] A. Oberlin, M. Endo, T. Koyama, Filamentous growth of carbon through benzene decomposition. *Journal of Crystal Growth*, Vol. 32 (3), pp. 335-349, 1975.

[45] R. Saito, G. Dresselhaus, M. S. Dresselhaus, *Physical Properties of Carbon Nanotubes*, World Scientific Publishing Company, 1998.

[46] S. Iijima, Helical microtubules of graphitic carbon. *Nature*, Vol. 354, pp. 56–58, 1991.

[47] P.M. Ajayan, L.S. Schadler, P.V. Braun, *Nanocomposite science and technology*, Wiley-VCH, 2003.

[48] J. H. Lehman, M. Terrones, E. Mansfield, K. E. Hurst, V. Meunier, Evaluating the characteristics of multiwall carbon nanotubes. *Carbon*, Vol. 49 (8), pp. 2581–2602, 2011.

[49] K. S. Ibrahim, Carbon nanotubes - properties and applications: a review. *Carbon Letters*, Vol. 14 (3), pp. 131–144, 2013.

[50] A. Tielas, B. Gabriel, C. Santos, D. Gracia, J. Alcorta, M. Blanchy, M. Blanco, O. Menes, S. Gálvez, V. Neto, *Nanomateriais - Guia para o espaço industrial SUDOE*, CarbonInspired 2.0, 2014.

[51] S. K. Kumar, N. Jouault, Nanocomposites with polymer grafted nanoparticles, *Macromolecules*, Vol. 46 (9), pp. 3199–3214, 2013.

[52] W. Qi, X. Zhang, H. Wang, Self-assembled polymer nanocomposites for biomedical application. *Current Opinion in Colloid and Interface Science*, Vol. 35, pp. 36–41, 2018.

[53] T. A. Saleh, P. Parthasarathy, M. Irfan, Advanced functional polymer nanocomposites and their use in water ultra-purification. *Trends in Environmental Analytical Chemistry*, Vol. 24, 2019.

[54] J. M. Raquez, Y. Habibi, M. Murariu, P. Dubois, Polylactide (PLA)-based nanocomposites. *Progress in Polymer Science*, Vol 38, pp. 1504–1542, 2013.

[55] C. Gonçalves, I. C. Gonçalves, F. D. Magalhães, A. M. Pinto, Poly(lactic acid) composites containing carbon-based nanomaterials: A review. *Polymers*, Vol. 9 (7), 2017.

[56] T. Villmow, P. Poetschke, S. Pegel, L. Haeussler, B. Kretzschmar, Influence of twin-screw extrusion conditions on the dispersion of multi-walled carbon nanotubes in a poly (lactic acid) matrix. *Polymer*, Vol. 49 (16), pp. 3500–3509, 2008.

[57] G. Postiglione, G. Natale, G. Griffini, M. Levi, S. Turri, Conductive 3D microstructures by direct 3D printing of polymer/carbon nanotube nanocomposites via liquid deposition modeling. *Composites: Part A*, Vol. 76, pp. 110–114, 2015.

[58] I. Armentano, N. Bitinis, E. Fortunati, S. Mattioli, N. Rescignano, et al, Multifunctional nanostructured PLA materials for packaging and tissue engineering. *Progress in Polymer Science*, Vol. 38, pp. 1720–1747, 2013.

[59] G. Oetjen, P. Haseley, *Freeze-Drying*, Wiley-VCH 3rd completely revised and enlarged edition, Weinheim, Germany, 2018.

[60] D. He, S. Mu, M. Pan, Improved carbon nanotube supported Pt nanocatalysts with lyophilization. *International Journal of Hydrogen Energy*, Vol. 37 (5), pp. 4699–4703, 2012.

[61] W. Abdelwahed, G. Degobert, S. Stainmesse, H. Fessi, Freeze-drying of nanoparticles: Formulation, process and storage considerations. *Advanced Drug Delivery Reviews*, Vol. 58 (15), pp. 1688–1713, 2006.

[62] J. Ahmed, S. K. Varshney, Polylactides-chemistry, properties and green packaging technology: A review. *International Journal of Food Properties*, Vol. 14 (1), pp. 37–58, 2011.

[63] K. M. Stridsberg, M. Ryner, A. C. Albertsson, Controlled ring-opening polymerization: Polymers with designed macromolecular architecture. *Advances in Polymer Science*, Vol. 157, pp. 41-65, 2001.

[64] ISO 527-2:1996 BS 2782-3: Method 322:1994, Plastics - Determination of tensile properties - Part 2: Test conditions for moulding and extrusion plastics, London South Bank University, 2006.

[65] G. dos Santos, *Análise do comportamento mecânico de componentes produzidos por Fabrico por Filamento Fundido*, Master's Thesis, University of Aveiro, 2016.

[66] S. Barrau, C. Vanmansart, M. Moreau, A. Addad, G. Stoclet, et al, Crystallization behavior of carbon nanotube-polylactide nanocomposites. *Macromolecules*, Vol. 44 (16), pp. 6496–6502, 2011.

[67] W.Y. Lin, Y.F. Shih, C.H. Lin, C.C. Lee, Y.H. Yu, The preparation of multi-walled carbon nanotube/poly(lactic acid) composites with excellent conductivity. *Journal of the Taiwan Institute of Chemical Engineers*, Vol 44(3), pp. 489–496, 2013.

[68] C.F. Kuan, H.C. Kuan, C.C.M. Ma, C.H. Chen, Mechanical and electrical properties of multi-wall carbon nanotube/poly(lactic acid) composites. *Journal of Physics and Chemistry of Solids*, Vol. 69, pp. 1395–1398, 2008.

[69] A.M. Ali, S. H. Ahmad, Mechanical characterization and morphology of polylactic acid/liquid natural rubber filled with multi walled carbon nanotubes. *AIP Conference Proceedings*, Vol. 1571, pp. 83–89, 2013.

[70] G. Gorrasi, A. Sorrentino, Photo-oxidative stabilization of carbon nanotubes on polylactic acid. *Polymer Degradation and Stability*, Vol. 98 (5), pp. 963–971, 2013.

[71] K. Gnanasekaran, T. Heijmans, S. van Bennekom, H. Woldhuis, S. Wijnia, et al, 3D printing of CNT- and graphene-based conductive polymer nanocomposites by fused deposition modelling. *Applied Materials Today*, Vol. 9, pp. 21–28, 2017.